

GENUS ONE SCHERK SURFACES AND THEIR LIMITS

CASEY DOUGLAS

This work is presented in memory of Connor Arellano Douglas

Abstract

The singly periodic, genus one helicoid was conjectured to be the limit of a one parameter family of doubly periodic minimal surfaces referred to as Perturbed Genus One Scherk Surfaces. Using elliptic functions, we show such surfaces exist, solving a two-dimensional period problem by perturbing a one-dimensional problem. Using flat structures associated to these minimal surfaces, we verify the conjecture.

1. Introduction

In this paper, we prove the existence of a one parameter family of doubly periodic minimal surfaces. The members of this family are embedded in \mathbb{R}^3 and their quotients have genus one and four vertical annular ends. We index this family by $\theta \in (0, \pi/2)$, where 2θ (and $\pi - 2\theta$) denotes the angle between the ends. We also show that as θ tends to zero (or $\pi/2$) these surfaces limit on the singly periodic genus one helicoid.

1.1. History. Our genus one surfaces can be visualized by attaching a handle to a fundamental piece of one of Scherk's doubly periodic surfaces. These classical surfaces are also parameterized by the angles at which their ends meet and can be defined by the Weierstrass data

$$g(z) = z$$

$$dh = iz \frac{dz}{(z - e^{i\theta})(z + e^{i\theta})(z - e^{-i\theta})(z + e^{-i\theta})}$$

The doubly periodic Scherk surface with orthogonal ends ($2\theta = \pi/2$) can also be described by the relation

$$e^z = \frac{\cos x}{\cos y}$$

and enjoys eight lines of symmetry. We refer to the other doubly periodic Scherk surfaces as “sheared” or “perturbed,” all of which possess two rotational symmetries.

Received 10/16/2009.

Using the techniques of Weber-Wolf [27] it can be shown that finitely but arbitrarily many handles may be added to Scherk's doubly periodic surface when the ends are perpendicular. Karcher [14] constructed a higher genus analog of Scherk's orthogonal doubly periodic surface by adding a handle in the most symmetric way possible; the technique that Weber-Wolf [27] later deployed also assumes maximal symmetry. In particular, the genus-one version of this surface is assumed to have a quotient that is conformally equivalent to a symmetrically punctured square torus.

Such assumptions have a particularly nice effect on the flat structure representations of the forms gdh and $(1/g)dh$. In fact, for the more general genus- g case, the flat structure representations are similarly easy to draw and work with, provided all of the handles are added in a symmetric fashion.

Let $S(g, 2\theta)$ denote a putative example of a perturbed genus- g Scherk surface whose ends meet at angles 2θ and $\pi - 2\theta$. Scherk [21] proved that for any $\theta \in (0, \pi/2)$ the surface $S(0, 2\theta)$ exists, and, as is shown in [23], if the parameter θ tends to 0 or $\pi/2$, these surfaces tend to a horizontal helicoid, one whose axis of revolution lies in the xy -plane. (Convergence is taken in the pointed Gromov-Hausdorff sense [8].) In other words

$$\lim_{\theta \rightarrow 0} S(0, 2\theta) = \mathcal{H}(0)$$

where $\mathcal{H}(0)$ denotes the singly periodic, genus zero helicoid.

Hoffman-Karcher-Wei [11] proved the existence of a singly periodic genus-one helicoid, which we denote by $\mathcal{H}(1)$. They were motivated by the suspicion that perturbed genus-one Scherk Surfaces, $S(1, 2\theta)$, exist for any $\theta \in (0, \pi/2)$, and that their limit should similarly exist, producing a singly periodic helicoid with a handle.

1.2. Main Results. The existence and uniqueness of $\mathcal{H}(1)$ is known (see [11], [3]) but establishing the existence of $S(1, 2\theta)$ was only recently accomplished by Batista-Ramos [4] via the method of the "support function." It remains unknown whether or not singly periodic, genus- g helicoids, denoted $\mathcal{H}(g)$, and $S(g, 2\theta)$ exist for $g > 1$ and $\theta \neq \pi/4$.

Unfortunately, the flat structure approach of Weber and Wolf does not seem to extend to $S(g, 2\theta)$ for arbitrary θ . Even for $g = 1$ their method is difficult to employ. Consequently, we aim to prove the existence of $S(1, 2\theta)$ for arbitrary θ by combining their techniques with basic elliptic function theory on rhombic tori. Our main result is the following

Theorem 1. *Given any $\theta \in (0, \pi/2)$, there exists a complete, embedded, doubly periodic minimal surface in \mathbb{R}^3 whose quotient has genus one and 4 Scherk-type ends meeting at angles 2θ and $\pi - 2\theta$.*

Moreover, as $\theta \rightarrow 0$ these surfaces limit on the singly periodic, genus one helicoid (in the pointed Gromov Hausdorff sense).

A portion of the orthogonal-ended surface, $S(1, \pi/2)$, is depicted on the left in Figure 1, while a portion of a sheared surface, $S(1, 2\theta)$ for some $\theta < \pi/4$, is depicted on the right.

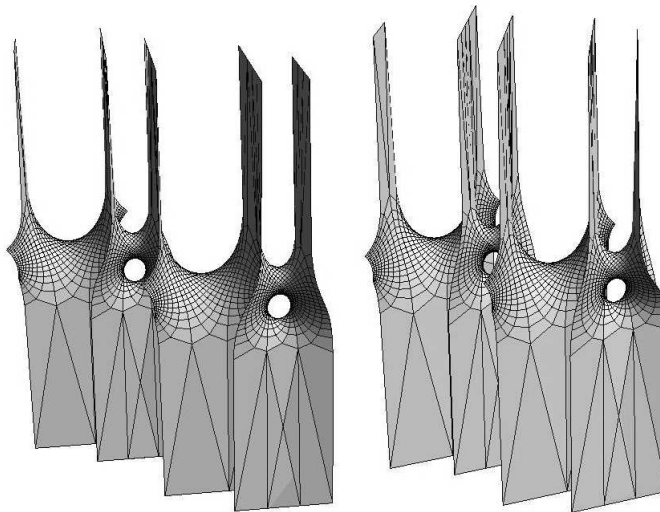


Figure 1. Orthogonal and sheared genus one scherk surfaces

Theorem 1 is proved in two main steps. First, it is shown that we can produce possibly perturbed surfaces $S(1, 2\theta)$ by deforming the underlying, symmetrically punctured rhombic torus off of the square torus. In addition to this toroidal deformation, we obtain a uniqueness result for $S(1, \pi/2)$. Using numerical estimates, Hauswirth-Traizet [10] argued that the surface $S(1, \pi/2)$ can be deformed in terms of θ , a result that is superior to this first step.

Next, we prove that this family of minimal surfaces has a limit. Using geometric coordinates that arise from flat structures, it is shown that this limit occurs when $\theta = 0$ or $\theta = \pi/2$, and that the resulting flat structures agree with those of the singly periodic, genus-one helicoid. This is enough to conclude that the surfaces converge to the singly periodic helicoid. A standard application of the maximum principle shows that the surfaces are embedded, finishing the the theorem.

Although the techniques underlying this proof depend, in part, on the genus being one, they are nonetheless encouraging in the interests of establishing the existence of $\mathcal{H}(g)$ for $g > 1$. One suspects that, as happens for $g = 0$ and $g = 1$, singly periodic helicoids with an arbitrary number of handles may be found by similarly perturbing the surfaces $S(g, \pi/2)$. That is, one suspects

$$\lim_{\theta \rightarrow 0} S(g, 2\theta) = \mathcal{H}(g).$$

1.3. An Outline of the Paper. In Section 2 we review the Weierstrass representation and the associated period problems for minimal surfaces. We also review facts about and notation for rhombic tori and their associated \wp functions.

Section 3 concerns necessary Weierstrass data for the proposed surface $S(1, 2\theta)$. We first collect expressions for and facts about g and dh . This data is parameterized by three real parameters (ϕ, θ, t) , where ϕ parameterizes the underlying rhombic torus and the pair (θ, t) determines where this torus is punctured. Next we address the vertical and horizontal period problems. After establishing that dh has no periods, we define the period function $F(\phi, \theta, t)$. This function vanishes if and only if the remaining horizontal period problem is solved.

The third subsection is devoted to proving Theorems 2 and 3, which assert our uniqueness and deformation results. In particular, we show the following

$$(1) \quad F(\pi/2, \theta, t) = 0 \iff (\theta, t) = (\pi/4, t_0)$$

$$(2) \quad \det |DF_{(\theta, t)}|_{(\pi/2, \pi/4, t_0)} > 0$$

where $t_0 \in (0, \infty)$. The Implicit Function Theorem then guarantees the existence of triples (ϕ, θ, t) near $(\pi/2, \pi/4, t_0)$ satisfying $F(\phi, \theta, t) = 0$.

In Section 4 we prove that the solution curve determined by $F(\phi, \theta, t) = 0$ is analytic so that Sullivan's Local Euler Characteristic Theorem [9] applies. As a result, this curve necessarily extends (with the possibility of branchings) to a boundary point where $\phi \in \{0, \pi\}$, $\theta \in \{0, \pi/2\}$, and/or $t \in \{0, \infty\}$.

We review the notions of extremal length and flat structures in Section 5. With these tools we show that the only allowable boundary points force the surfaces $S(1, 2\theta)$ to limit on the singly periodic, genus-one helicoid, $\mathcal{H}(1)$. Lastly, we argue that these surfaces are all necessarily embedded.

2. Preliminaries

2.1. Minimal Surfaces. There are a number of ways to define a minimal surface (see, for example, [7] or [13]), but one of the more common or useful formulations involves **Weierstrass data**. A result of Osserman tells us that every finite total curvature minimal surface is conformally a compact Riemann surface with finitely many punctures [19]. The map $X : \mathcal{R} \rightarrow \mathbb{R}^3$ that parameterizes our Riemann surface, \mathcal{R} , as a minimal surface admits an integral representation that is given by

$$X(z) = \operatorname{Re} \int^z \left(\frac{1}{2} \left(\frac{1}{g} + g \right) dh, \frac{i}{2} \left(\frac{1}{g} - g \right) dh, dh \right).$$

Here g is a meromorphic function, dh is a holomorphic 1-form, and z is a local coordinate on the punctured surface \mathcal{R} . The pair (g, dh) is referred to as the Weierstrass data for the minimal surface.

Both g and dh have geometric significance. As the notation suggests, dh is the (complexified) differential of the height function, and g is the Gauss map composed with stereographic projection. To construct a desired minimal surface, it suffices to determine appropriate g and dh . In order for the surface to be unbranched, one first has to ensure that the zeroes and poles of g agree with the zeroes of dh . In order for the map X to be well defined, one has to solve the period problem(s)

$$\begin{aligned} \operatorname{Re} \left(\int_{\gamma} \frac{1}{2} \left(\frac{1}{g} + g \right) dh \right) &= 0 \\ \operatorname{Re} \left(\int_{\gamma} \frac{i}{2} \left(\frac{1}{g} - g \right) dh \right) &= 0 \\ \operatorname{Re} \left(\int_{\gamma} dh \right) &= 0 \end{aligned}$$

where the integrals are taken over all generators γ of $H_1(\mathcal{R}; \mathbb{C})$. The first two equations are often referred to as the horizontal period problem, while the last is the vertical period problem. The horizontal period problem can be rewritten as a single complex equation

$$\int_{\gamma} g dh = \overline{\int_{\gamma} \frac{1}{g} dh}$$

again for all γ that generate $H_1(\mathcal{R}; \mathbb{C})$. If \mathcal{R} has genus k and n punctures, there are $3(2k+n-1)$ real conditions to satisfy. Moreover, if \mathcal{R} has high genus, then the function g and 1-form dh can be difficult to determine. In summary, topologically complicated minimal surfaces are often difficult to construct via Weierstrass data.

When \mathcal{R} is a punctured sphere, the period problem typically reduces to a condition on the residues of $g dh$, $(1/g)dh$ and dh , namely that they are purely real. A good example has already been mentioned: Scherk's doubly periodic surface, which is defined on $\hat{\mathbb{C}} - \{\pm e^{\pm i\theta}\}$ by the data

$$\begin{aligned} g(z) &= z \\ dh &= \frac{iz dz}{\prod (z \pm e^{\pm i\theta})} \end{aligned}$$

Only the vertical period problem is solved for this data, producing a doubly periodic surface in \mathbb{R}^3 that is defined over the lattice generated by $(\sec \theta, \csc \theta, 0)$ and $(-\sec \theta, \csc \theta)$. For many other examples, consult [24].

2.2. The Weierstrass \wp Function for Rhombic Tori. Let Λ_ϕ denote the rhombic lattice generated by $\{1, e^{i\phi}\}$. The Weierstrass \wp function for the torus \mathbb{C}/Λ_ϕ is given by

$$\wp(z) = \frac{1}{z^2} + \sum_{n,m \in \mathbb{Z}^*} \frac{1}{(z - n - e^{i\phi}m)^2} - \frac{1}{(n + e^{i\phi}m)^2}$$

The symmetries of the lattice produce symmetries within the \wp function. Specifically, reflecting across either line of symmetry is given by

$$\begin{aligned} z &\mapsto e^{i\phi}\bar{z} \\ z &\mapsto 1 + e^{i\phi} - e^{i\phi}\bar{z} \end{aligned}$$

and the values of \wp change according to the formulae

$$\begin{aligned} \wp(e^{i\phi}\bar{z}) &= e^{-2i\phi}\overline{\wp(z)} \\ \wp(1 + e^{i\phi} - e^{i\phi}\bar{z}) &= \wp(e^{i\phi}\bar{z}) = e^{-2i\phi}\overline{\wp(z)}. \end{aligned}$$

In fact, the following, more general formulae holds for any k -th order derivative of \wp :

$$\begin{aligned} \wp^{(k)}(e^{i\phi}\bar{z}) &= e^{-(2+k)i\phi}\overline{\wp^{(k)}(z)} \\ \wp^{(k)}(-e^{i\phi}\bar{z}) &= (-1)^k e^{-(2+k)i\phi}\overline{\wp^{(k)}(z)}. \end{aligned}$$

We list some notation and collect elementary facts about the \wp function for the rhombic torus \mathbb{C}/Λ_ϕ :

$$\begin{aligned} \omega_1 &= 1/2, \quad \omega_2 = e^{i\phi}/2, \quad \omega_3 = \omega_1 + \omega_2 \\ e_i &= \wp(\omega_i) \\ (\wp')^2 &= 4(\wp - e_1)(\wp - e_2)(\wp - e_3) \\ e_2 &= e^{-2i\phi}\overline{e_1} \\ e_1 &= e^{-2i\phi}\overline{e_2} \\ 0 &= e_1 + e_2 + e_3 \\ e_3 &= 2e^{-i\phi}\operatorname{Re}(e^{i\phi}e_1) \Rightarrow e_3 \in e^{-i\phi}\mathbb{R} \\ e_3 = 0 &\iff \phi = \pi/2 \\ \wp(z) \in e^{-i\phi}\mathbb{R} &\iff z \text{ lies on a diagonal} \end{aligned}$$

From the last equation, we immediately conclude that the zeroes of the \wp function lie along a diagonal. For more information on \wp see [6].

2.3. The Square Torus. On the square torus \wp is real valued along the horizontal and vertical lines bordering the fundamental square and along the dividing lines $x = 1/2$ and $y = 1/2$. It is purely imaginary along the two diagonals.

The derivative, \wp' , is real valued along the horizontal lines $y = 0$ and $y = 1/2$ and it is imaginary along the vertical lines $x = 0$ and $x = 1/2$. It takes values in $e^{i\pi/4}\mathbb{R}$ along the diagonals.

It is straightforward to see that along the real axis \wp has as its minimum value the number $e_1 = \wp(\omega_1)$.

3. The Initial Surface $S(1, \pi/2)$ and Toroidal Deformations

Here we prove that $S(1, \pi/2)$ exists, which is not a new result (see [14] and [26]). However, the methods we use offer a slight improvement on previous results; specifically, we show that up to a re-indexing of data and a shift and rotation of the torus, there is only one way to puncture the square torus so that it embeds as $S(1, \pi/2)$. Moreover, the punctures are placed only with respect to the torus' rhombic symmetry, whereas in previous constructions the punctures were placed with respect to both rhombic and rectangular symmetry lines. This is the content of Theorem 2.

Next, the Implicit Function Theorem is used to show that for ϕ sufficiently close to $\pi/2$, one can puncture the torus \mathbb{C}/Λ_ϕ so that the resulting surface immerses into \mathbb{R}^3 as $S(1, 2\theta)$ for some $\theta \in (0, \pi/2)$. This is the content of Theorem 3.

Theorems 2 and 3 are achieved via the period functions $F(\phi, \theta, t)$ and $\hat{F}(\phi, \theta, t)$, which detect when the horizontal period problem is solved. These function use expressions for g and dh which we collect in the proceeding subsection; these expressions are parameterized by three real variables (ϕ, θ, t) and one complex variable $s = s(\phi, \theta, t)$ that depends on the others.

3.1. Expressions for g and dh . Based on computer images (see [12]) we expect $S(1, 2\theta)$ to possess two rotational symmetries, each of which interchange two ends and maintain the set of vertical points. Near the ends, the function g and the one-form dh should behave like the Gauss map and height differential for $S(0, 2\theta)$; that is, g should be horizontal at these points and dh should have simple poles with residues given by the residues of the height-differential for the genus-0 surface.

All of this, along with an analysis of the connectivity of the fixed point set of the reflections, imply that $S(1, 2\theta)$ is conformally equivalent to a symmetrically punctured rhombic torus, $\mathbb{C}/\Lambda_\phi - \{a_1, \dots, a_4\}$ whose Weierstrass data satisfy the following divisor table:

	0	ω_1	ω_2	ω_3	a_1	a_2	a_3	a_4
dh	0	0	0	0	∞	∞	∞	∞
g	0	∞	∞	0	$e^{i\theta}$	$e^{-i\theta}$	$-e^{i\theta}$	$-e^{-i\theta}$

The behavior of the height differential for $S(0, 2\theta)$ near the ends determines the behavior of dh for $S(1, 2\theta)$ near *its* ends; specifically, dh must

have purely real residues given by

$$\operatorname{Res}_{a_3} = \operatorname{Res}_{a_1} dh = \frac{\sec \theta \csc \theta}{8} = -\operatorname{Res}_{a_2} dh = -\operatorname{Res}_{a_4} dh$$

As indicated by the above table, the Gauss map must take on the values $\pm e^{\pm i\theta}$ (with multiplicity 1) at the punctures a_i . This is enough information to determine the data (g, dh) up to a multiplicative factor. In fact, the symmetric placement of the punctures,

$$\begin{aligned} a_2 &= e^{i\phi} \overline{a_1} \\ a_3 &= 1 + e^{i\phi} - a_1 \\ a_4 &= 1 + e^{i\phi} - a_2 \end{aligned}$$

allows us to express g and dh as

$$\begin{aligned} g(z) &= \frac{t}{e^{i\phi/2}} \cdot \frac{\wp - e_3}{\wp'} \\ dh &= \frac{\wp(a_1) - \wp(a_2)}{8 \sin \theta \cos \theta} \cdot \frac{d\wp}{(\wp - \wp(a_1))(\wp - \wp(a_2))} \\ &= ie^{-i\phi} \frac{\operatorname{Im}(e^{i\phi} \wp(a_1))}{4 \sin \theta \cos \theta} \cdot \frac{d\wp}{(\wp - \wp(a_1))(\wp - \wp(a_2))}. \end{aligned}$$

The last expression for dh was obtained by using the reflection rule

$$\wp(a_2) = \wp(e^{i\phi} \overline{a_1}) = e^{-2i\phi} \overline{\wp(a_1)}.$$

The variable t takes values in $t \in (0, \infty)$. More to the point, given a triple (ϕ, θ, t) , we can construct the Gauss map g on the torus \mathbb{C}/Λ_ϕ . We then puncture said torus at the points a_i where $g(a_i) = \pm e^{\pm i\theta}$, which allows us to construct dh . It is easy to see that g is a degree 2 map, and so there are two possible choices for each of the a_i ; there is also ambiguity in the ordering of the points a_i . Via the following propositions, we can normalize these choices. We also point out that the Gauss map is purely real along one diagonal and purely imaginary along the other, and that it is an odd map.

Proposition 1. *Again, let g denote the Gauss map for the rhombic torus \mathbb{C}/Λ_ϕ . Then $g(z)$ satisfies $g(z) = g(\omega_3 - z)$.*

Proof. Naturally, it suffices to check this claim for the map $(\wp - e_3)(\wp')^{-1}$. Again, this follows after analyzing the divisor data for the two maps

$$g_1(z) = \frac{\wp(z) - e_3}{\wp'(z)}, \quad g_2(z) = \frac{\wp(\omega_3 - z) - e_3}{\wp'(\omega_3 - z)} = g_1(\omega_3 - z)$$

Both g_1 and g_2 have simple zeroes at 0 and at ω_3 and both have simple poles at ω_1 and ω_2 . From this we conclude that $g_1(z) = C \cdot g_1(\omega_3 - z)$.

To determine that $C = 1$ simply evaluate both functions at $z = \omega_3/2$.
q.e.d.

Proposition 2. *The Gauss map has 4 ramification points located along the diagonals, halfway between the vertices of the rhombus and the center ω_3 .*

Proof. Every elliptic, degree 2 meromorphic function has 4 ramification points (with index 2 at each point), and to determine the location of these points we appeal to the previous proposition. The points so described in the hypothesis are invariant (mod $\{1, e^{i\phi}\}$) under the action $z \mapsto \omega_3 - z$, and since the previous proposition implies $g'(\omega_3 - z) = -g'(z)$, the proof is done. q.e.d.

Proposition 3. *The triple $(\phi, \theta, t) \in (0, \pi) \times (0, \pi/2) \cup (-\pi/2, 0) \times \mathbb{R}^+$ determines the same punctured torus that the triples $(\phi, \theta, -t)$ and $(\phi, -\theta, t)$ determine, modulo a re-indexing of the punctures and a possible shift and/or 180° rotation of the torus.*

Proof. Since ϕ determines the torus, we only need to check that (θ, t) , $(\theta, -t)$, and $(-\theta, t)$ determine the same punctures up to re-ordering and a possible shift and rotation of the torus. Let $t \in \mathbb{R}^+$ and $\theta \in (0, \pi/2)$ be given. The Gauss map is a degree 2, branched cover over the sphere, $\hat{\mathbb{C}}$, that, by the previous claim, is ramified at points along the diagonals where it is purely real or purely imaginary. Since $\theta \neq 0$ and $\theta \neq \pm\pi/2$ the point $e^{i\theta}$ has two pre-images under the map g :

$$g^{-1}\{e^{i\theta}\} = \{a_1, b_1\}$$

From the first claim, we suspect that $b_1 \equiv \omega_3 - a_1$, but we need to make sure that $\omega_3 - a_1$ and a_1 are distinct points in the torus. This is immediate, though, since $a_1 \equiv \omega_3 - a_1 \iff 2a_1 \equiv \omega_3 \iff a_1$ lies along a diagonal, which cannot happen since we are assuming that $g(a_1) = e^{i\theta}$, which is neither real nor imaginary. Therefore, we may obtain one pre-image from the other by shifting and rotating the torus.

Without loss of generality, choose the puncture to be a_1 . Because g is odd and because $a_3 = 1 + e^{i\phi} - a_1 \equiv -a_1$ we have that $g(a_3) = -e^{i\theta}$. This implies that the triple $(\phi, \theta, -t)$ corresponds to relabeling $a_3 \mapsto a_1$ or $b_3 \mapsto a_1$, the first of which is a simple re-indexing of the punctures, the second a shift and rotation followed by a re-indexing.

Similarly, the choice $(\phi, -\theta, t)$ corresponds to relabeling $a_2 \mapsto a_1$ or $b_2 \mapsto a_1$, which completes the proof. q.e.d.

We also note that the map $(\wp')(\wp - e_3)^{-1}$ takes two curves to the double ray $e^{-i\phi/2}e^{i\theta}\mathbb{R}$, call them γ_1 and γ_2 , where γ_1 joins ω_3 to ω_1 and γ_2 joins ω_2 to 0. Hence, the Gauss map g takes these curves to the ray $e^{i\theta}\mathbb{R}$. A straightforward reflection argument shows that the curves γ_i are contained in the shaded boxes depicted in Figure 2. In particular,

they cannot cross the boundary of the parallelogram (except at ω_1 and ω_2) representing the rhombic torus.

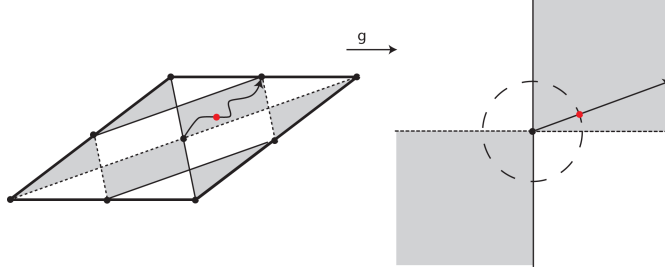


Figure 2. Gauss map

We further normalize the situation by agreeing to label a_1 as the pre-image of $e^{i\theta}$ under g , and we agree to puncture the torus at a_1 and its reflections.

The Gauss map g is purely real and imaginary along the diagonals and the lines indicated in Figure 2, and these are the only places where g takes on such values. As a result, for $\theta \neq 0$ or $\theta \neq \pi/2$, the punctures a_i must be chosen to lie in the interiors of the shaded boxes in Figure 1.

3.1.1. One More Parameter. Because our expression for dh involves $\wp(a_1)$ —where a_1 is determined by a choice for the triple (ϕ, θ, t) and our normalizing conditions—it will be beneficial to treat this value as another variable. That is, we label

$$\begin{aligned} s &= \wp(a_1) \\ \bar{s}e^{-2i\phi} &= \wp(a_2). \end{aligned}$$

We derive an explicit relationship between s and the triple (ϕ, θ, t) that results from the differential equation satisfied by \wp :

$$\begin{aligned} \frac{\wp'(a_1)}{\wp(a_1) - e_3} &= \frac{\wp'(a_1)}{s - e_3} = \frac{t}{e^{i\theta} e^{i\phi/2}} \\ \Rightarrow \frac{\wp'(a_1)^2}{(s - e_3)^2} &= 4 \frac{(s - e_1)(s - e_2)}{(s - e_3)} = \frac{t^2}{e^{2i\theta} e^{i\phi}} \\ 4e^{2i\theta} e^{i\phi} (s - e_1)(s - e_2) - t^2 (s - e_3) &= 0. \end{aligned}$$

This equation, along with our normalizing conditions, implicitly defines s as a function of our parameters, $s = s(\phi, \theta, t)$. Later we will show that $s(\phi, \theta, t)$ depends analytically on $(\phi, \theta, t) \in \mathcal{P}$, where \mathcal{P} is our parameter space given by the open half-slab $\mathcal{P} = (0, \pi) \times (0, \pi/2) \times (0, \infty)$. We now rewrite our expressions for g and dh one last time and collect expressions for gdh and $(1/g)dh$:

$$\begin{aligned}
g &= \frac{t}{e^{i\phi/2}} \cdot \frac{\wp - e_3}{\wp'} = e^{i\theta} \frac{\wp'(a_1)}{s - e_3} \cdot \frac{\wp - e_3}{\wp'} \\
dh &= ie^{-i\phi} \frac{\operatorname{Im}(e^{i\phi}s)}{4 \sin \theta \cos \theta} \cdot \frac{d\wp}{(\wp - s)(\wp - \bar{s}e^{-2i\phi})} \\
gdh &= ie^{-3i\phi/2} \cdot t \frac{\operatorname{Im}(e^{i\phi}s)}{4 \sin \theta \cos \theta} \cdot \frac{\wp - e_3}{(\wp - s)(\wp - \bar{s}e^{-2i\phi})} dz \\
\frac{dh}{g} &= ie^{-i\phi/2} \cdot \frac{1}{t} \cdot \frac{\operatorname{Im}(e^{i\phi}s)}{4 \sin \theta \cos \theta} \cdot \frac{4(\wp - e_1)(\wp - e_2)}{(\wp - s)(\wp - \bar{s}e^{-2i\phi})} dz
\end{aligned}$$

3.2. The Period Problem. Symmetries and residues reduce what should be a 5-dimensional (real) period problem to a 2-dimensional one. In the case of the square torus, additional symmetry cuts this down to a 1-dimensional problem.

3.2.1. The Periods of dh . A straightforward computation confirms that the residues of dh are purely real; specifically, they are given by $\pm(1/8) \sec \theta \csc \theta$. Along paths γ_i that enclose our punctures a_i we therefore have

$$\int_{\gamma_i} dh = \frac{\pm 2\pi i}{8 \sin \theta \cos \theta} \in i\mathbb{R}$$

The bilinear relation applied to $dz \wedge dh$ then yields

$$0 = \iint_{\mathcal{R}} dz \wedge dh = \int_1^0 dz \int_0^{e^{i\phi}} dh - \int_0^{e^{i\phi}} dz \int_1^0 dh + 2\pi i \sum_{i=1}^4 a_i \operatorname{Res}_{a_i} dh$$

where \mathcal{R} is a parallelogram representing our torus, with vertices $0, 1, e^{i\phi}$, and $1 + e^{i\phi}$.

The residue sum above vanishes, leaving the equation

$$e^{i\phi} \int_0^1 dh = \int_0^{e^{i\phi}} dh.$$

From this we conclude that *if* dh is to have purely imaginary periods, then the integrals above must vanish. Otherwise we are forced to conclude that $e^{i\phi} \in \mathbb{R}$ which gives us a degenerate torus.

Proposition 4. *Let $H(z) : \mathbb{C}/\Lambda_\phi \rightarrow \mathbb{C}$ be an odd function. If the periods of $H(z)dz$ are integrable, then they vanish.*

Proof. Let β_1 be the path parameterized by $z(t) = t$ for $t \in [0, 1]$, and let β_2 be parameterized by $w(t) = 1 + e^{i\phi} - z(t)$. The double-periodicity

of H and difference in direction between β_1 and β_2 imply

$$\begin{aligned} \int_{\beta_1} H(z)dz &= - \int_{\beta_2} H(w)dw \\ \int_0^1 H(t)dt &= - \int_0^1 H(1 + e^{i\phi} - t)dw(t) = \int_0^1 H(1 + e^{i\phi} - t)dt \\ &= - \int_0^1 H(t)dt \\ \Rightarrow \int_{\beta_1} H(z)dz &= 0. \end{aligned}$$

Similar computations reveal that the integral of H along the remaining perimeter curve vanishes. q.e.d.

This allows us to conclude that there is no period problem for dh , for $dh = H(z)dz$ where $H(z)$ is odd. The above proposition then applies. If we let β_1 and β_2 denote the generators for $H_1(\mathbb{C}/\Lambda_\phi)$, then the first homology group for our punctured torus is generated by $\beta_1, \beta_2, \gamma_i$ where each γ_i encloses a puncture. Since the integral of dh vanishes along the β_i and is purely imaginary along the γ_i , the integral of dh along *any* cycle is purely imaginary.

3.2.2. The Periods of gdh and $(1/g)dh$. A careful but straightforward examination of the forms gdh and $(1/g)dh$ and their behavior under reflection reveals

$$\begin{aligned} \int_{\beta_1} gdh &= - \overline{\int_{\beta_2} gdh} \\ \int_{\beta_1} \frac{1}{g}dh &= - \overline{\int_{\beta_2} \frac{1}{g}dh} \end{aligned}$$

where β_1 and β_2 are straight lines joining the origin to the points 1 and $e^{i\phi}$, respectively. As a result, we see that the horizontal period condition is solved along $\beta_1 \iff$ it is solved along β_2 .

It is also easily verified that along γ_i the period condition fails in accordance with the desired double-periodicity of the surface; this follows from having set the residues of dh and values of g at the punctures equal to the residues and values of the Weierstrass data for the genus 0 surface.

3.2.3. The Period Function. Because the form dh has no periods, we will have an immersed, minimal surface with all of the desired properties, provided we can solve the remaining horizontal period problem. The aforementioned symmetry requires that we only solve this problem along either β_1 or β_2 ; in other words, we will have our desired minimal surface

provided

$$\int_0^1 g dh = \int_0^1 \frac{1}{g} dh.$$

Using our expressions for g and dh this equation simplifies significantly, yielding

$$\begin{aligned} & |s - e_1||s - e_2| \int_0^1 \frac{\wp - e_3}{(\wp - s)(\wp - \bar{s}e^{-2i\phi})} dx \\ &= -|s - e_3|e^{2i\phi} \int_0^1 \frac{(\bar{\wp} - \bar{e}_1)(\bar{\wp} - \bar{e}_2)}{(\bar{\wp} - \bar{s})(\bar{\wp} - \bar{s}e^{-2i\phi})} dx \end{aligned}$$

Define the **Period Function** for the triple (ϕ, θ, t) by the difference of these two expressions. That is, let

$$\begin{aligned} F(\phi, \theta, t) &= |s - e_1||s - e_2| \int_0^1 \frac{\wp - e_3}{(\wp - s)(\wp - \bar{s}e^{-2i\phi})} dx \\ &+ |s - e_3|e^{2i\phi} \int_0^1 \frac{(\bar{\wp} - \bar{e}_1)(\bar{\wp} - \bar{e}_2)}{(\bar{\wp} - \bar{s})(\bar{\wp} - \bar{s}e^{-2i\phi})} dx \end{aligned}$$

Proposition 5. *For any $\phi \in (0, \pi)$ and any $\theta \in [0, \pi/2]$, we have*

$$\begin{aligned} F(\phi, \theta, 0) &= |e_1 - e_3|e^{2i\phi} = |e_2 - e_3|e^{2i\phi} \\ F(\phi, \theta, \infty) &= |e_3 - e_1||e_3 - e_2| \int_0^1 \frac{dz}{\wp - e_3} \end{aligned}$$

Proof. First, observe that because of the equation

$$4e^{2i\theta}e^{i\phi}(s - e_1)(s - e_2) - t^2(s - e_3) = 0$$

the parameter $t = \infty \iff s = e_3$, and $t = 0 \iff s = e_1$ or $s = e_2$. We obtain the equations above simply by evaluating the period function at $s = e_3$ and $s = e_1$ or e_2 . However, the first integrand in our expression for F has singularities when $s = e_1$ and $s = e_2$, and so more care is needed to perform the evaluation at these points.

We only need to check that the first integral vanishes when taken over a small neighborhood of the point $1/2$. Outside of this neighborhood, the integrand is bounded even as $s \rightarrow e_1$, and since the coefficient tends to 0 as this happens, the entire expression vanishes. Now, over an interval $[1/2 - \delta, 1/2 + \delta]$ we use a result from [5] to conclude that what remains

similarly tends to 0 as $s \rightarrow e_1$. One finds

$$\begin{aligned} & \left| \int_{\frac{1}{2}-\delta}^{\frac{1}{2}+\delta} \frac{\wp - e_3}{(\wp - s)(\wp - \bar{s}e^{-2i\phi})} dx \right| \sim \left| M \int_{\frac{1}{2}-\delta}^{\frac{1}{2}+\delta} \frac{dx}{(\wp - s)} \right| \\ &= \left| M \int_{\frac{1}{2}-\delta}^{\frac{1}{2}+\delta} \frac{dx}{(\wp - \wp(a_1))} \right| \\ &= |M| \left| \frac{1}{\wp'(a_1)} \left[\ln \frac{\sigma(x - a_1)}{\sigma(x + a_1)} + 2x\zeta(a_1) \right] \right|_{\frac{1}{2}-\delta}^{\frac{1}{2}+\delta} \end{aligned}$$

where $\zeta(x) = -\int \wp(x)dx$, $\sigma(x) = e^{\int \zeta(x)dx}$, and M is constant. If we let $a_1 \rightarrow \omega_1 = 1/2$, the above expression vanishes when we multiply it by the coefficient $|s - e_1|$. q.e.d.

3.3. The Existence and Uniqueness of $S(1, \pi/2)$ and Toroidal Deformations. We now state our two main theorems and outline a strategy for their proof:

Theorem 2. *The function $F(\pi/2, \theta, t) = 0 \iff \theta = \pi/4$ and $t = t_0 \in (0, \infty)$, where t_0 is uniquely determined. In particular, there is only one way to puncture the square torus with respect to its rhombic symmetry (modulo our normalizing conditions) so that it immerses as $S(1, 2\theta)$; moreover, it must immerse as $S(1, \pi/2)$.*

Our strategy for proving Theorem 2 is straightforward. We show that the imaginary part of $F(\pi/2, \theta, t)$ vanishes if and only if $s \in \mathbb{R}$ which, when coupled with our normalizing conditions, forces $\theta = \pi/4$, which in turn forces s to be real. The Intermediate Value Theorem is used to show that the real part of this function vanishes for some choice of s , and hence for some choice of t . Finally, derivative estimates show that this real part is monotone in s , establishing uniqueness.

Theorem 3. *For ϕ sufficiently close to $\pi/2$ there exists a pair $(\theta, t) \in (0, \pi/2) \times (0, \infty)$ so that $F(\phi, \theta, t) = 0$.*

Our strategy for proving Theorem 3 is outlined in two steps:

- (1) Prove that $D\hat{F}_{(\theta, t)}$ has full rank at the point $(\pi/2, \pi/4, t_0)$ where $F = |s - e_3| \cdot \hat{F}$ relates the two functions. Again, we rely heavily on the Weierstrass \wp function for the square torus to prove this claim.
- (2) Use the relationship between $D\hat{F}$ and DF to conclude that $DF_{(\theta, t)}$ has full rank at the point $(\pi/2, \pi/4, t_0)$. Lastly, appeal to the implicit function theorem to ensure the existence of (θ, t) , solving the period problem near $\phi = \pi/2$.

Remark. Our proof of Theorem 3 will actually demonstrate that $\theta(\phi)$ and $t(\phi)$ depend smoothly on ϕ near $\phi = \pi/2$.

3.3.1. Proof of Theorem 2. Setting $\phi = \pi/2$ simplifies our period function F . In this situation $-e_2 = e_1 > 0$ and $e_3 = 0$. As a result $\bar{s}e^{-2i\phi} = -\bar{s}$ and

$$F(\pi/2, \theta, t) = |s^2 - e_1^2| \int_0^1 \frac{\wp}{(\wp - s)(\wp + \bar{s})} dx - |s| \int_0^1 \frac{\bar{\wp}^2 - \bar{e}_1^2}{(\bar{\wp} - \bar{s})(\bar{\wp} + s)} dx$$

Because this expression depends only on s we denote $F(\pi/2, \theta, t) = F(s)$. Moreover, because \wp is real valued along the interval $[0, 1]$ we may omit all of the conjugation in the second integral (except over s), yielding

$$F(s) = |s^2 - e_1^2| \int_0^1 \frac{\wp}{(\wp - s)(\wp + \bar{s})} dx - |s| \int_0^1 \frac{\wp^2 - e_1^2}{(\wp - \bar{s})(\wp + s)} dx$$

A solution will exist precisely when we find a value of s so that $\text{Re}(F(s)) = \text{Im}(F(s)) = 0$. Let us examine the latter condition first, computing the imaginary parts of each integrand.

$$\begin{aligned} & \text{Im} \left(\frac{\wp(x)}{(\wp(x) - s)(\wp(x) + \bar{s})} \right) \\ &= \frac{\wp(x)}{|\wp(x) - s|^2 |\wp(x) + \bar{s}|^2} \text{Im}((\wp(x) - \bar{s})(\wp(x) + s)) \\ &= \frac{2\wp^2(x)}{|\wp(x) - s|^2 |\wp(x) + \bar{s}|^2} \text{Im}(s) \end{aligned}$$

A similar computation reveals that the imaginary part of the second integrand is equal to

$$\frac{-2\wp(x)(\wp^2(x) - e_1^2)}{|\wp(x) - \bar{s}|^2 |\wp(x) + s|^2} \text{Im}(s)$$

Together we have the equation

$$\begin{aligned} & \text{Im}(F(s)) \\ &= 2 \left(|s^2 - e_1^2| \int_0^1 \frac{\wp^2}{|\wp - s|^2 |\wp + \bar{s}|^2} dx + |s| \int_0^1 \frac{\wp(\wp^2 - e_1^2)}{|\wp - \bar{s}|^2 |\wp + s|^2} dx \right) \text{Im}(s) \end{aligned}$$

We claim that the terms of the sum are both positive and finite. This is evident for the first term, and for the second term one simply needs to recall that the value e_1 is a local minimum for the real valued function $\wp(x)$ along the segment $[0, 1]$.

We see that when $\phi = \pi/2$ the period function satisfies $\text{Im}(F(s)) = 0 \iff \text{Im}(s) = 0$. In other words, the parameter $\wp(a_1) = s$ is strictly real, and this forces the puncture to lie along any of the lines that border the fundamental square, or along any of the dividing lines $x = 1/2$ or $y = 1/2$. Already, this forces $\theta = \pm\pi/4$ since s satisfies

$$4ie^{2i\theta}(s^2 - e_1^2) = t^2 s$$

As $s^2 - e_1^2$ and $t^2 s$ are both real, we have no other choices for θ . Moreover, our other normalizing condition—that a_1 be chosen along the curve γ_1 —forces us to pick $|s| = s \in (0, e_1)$. This simplifies our expression for $F(s)$ even more:

$$F(s) = (e_1^2 - s^2) \int_0^1 \frac{\wp}{\wp^2 - s^2} dx - s \int_0^1 \frac{\wp^2 - e_1^2}{\wp^2 - s^2} dx$$

The period function we are now left with is differentiable in s as the variable ranges over $(0, e_1)$. In order to find that $F(s) = \operatorname{Re}(F(s)) = 0$ we only appeal to the period function's continuity in s . Specifically, since

$$F(0) = e_1^2 \int_0^1 \frac{dz}{\wp} > 0$$

and $F(e_1) = -e_1 < 0$, we have the existence of a point s_0 where $F(s) = 0$. Denote this value of s by s_0 .

A priori, there could be multiple choices of a_1 (or, equivalently, s) that satisfy $\operatorname{Re}(F(s)) = F(s) = 0$. A straightforward calculus-based argument shows that s_0 is unique. Differentiating $F(s)$ with respect to s yields

$$\begin{aligned} F'(s) &= -2s \int_0^1 \frac{\wp}{\wp^2 - s^2} dx + 2s(e_1^2 - s^2) \int_0^1 \frac{\wp}{(\wp^2 - s^2)^2} dx \\ &\quad - \int_0^1 \frac{\wp^2 - e_1^2}{\wp^2 - s^2} dx - 2s^2 \int_0^1 \frac{\wp^2 - e_1^2}{(\wp^2 - s^2)^2} dx \end{aligned}$$

It is not difficult to argue that $F'(s) < 0$. We first note that as $0 < s < e_1 < \wp(x)$ for all $x \in [0, 1]$, all of the integrands in the above expression are positive. This would seal the deal were it not for the second integral term, whose coefficient is positive. Instead what we argue is that the first term is larger in modulus than the second term. Specifically, we claim

$$2s \int_0^1 \frac{\wp}{\wp^2 - s^2} dx > 2s(e_1^2 - s^2) \int_0^1 \frac{\wp}{(\wp^2 - s^2)^2} dx$$

Canceling a $2s$ from both sides we see that it suffices to prove

$$\frac{\wp(x)}{\wp(x)^2 - s^2} > (e_1^2 - s^2) \frac{\wp(x)}{(\wp(x)^2 - s^2)^2}$$

for all $s \in (0, e_1)$ and all $x \in [0, 1]$. Again, this follows from the fact that \wp has a minimum at e_1 along the segment $[0, 1]$.

$$\begin{aligned}
\wp^2(x) - s^2 &\geq e_1^2 - s^2 \\
\Rightarrow \frac{1}{\wp(x)^2 - s^2} &\leq \frac{1}{e_1^2 - s^2} \\
\Rightarrow (e_1^2 - s^2) \frac{\wp(x)}{(\wp(x)^2 - s^2)(\wp(x)^2 - s^2)} &\leq \frac{\wp(x)}{\wp(x)^2 - s^2}
\end{aligned}$$

As a result, the function $F(s)$ is monotone decreasing on $(0, e_1)$, and this completes our proof. In fact, this says a bit more than we set out to prove; for $\phi = \pi/2$ there is precisely one pair $(\theta, t) = (\pi/4, t_0)$ satisfying $F(\pi/2, \pi/4, t_0) = 0$. q.e.d.

3.3.2. Proof of Theorem 3. Differentiating the period function with respect to θ and t is going to result in unappealing formulae. To simplify matters, we instead work with the function

$$t^2 \int_0^1 \frac{\wp - e_3}{(\wp - s)(\wp - \bar{s}e^{-2i\phi})} dx + 4e^{2i\phi} \int_0^1 \frac{(\bar{\wp} - \bar{e}_1)(\bar{\wp} - \bar{e}_2)}{(\bar{\wp} - \bar{s})(\bar{\wp} - se^{2i\phi})} dx.$$

Technically this is a different function, but it agrees with F up to a positive, multiplicative factor. We name this function \hat{F} and note

$$F(\phi, \theta, t) = |s - e_3| \cdot \hat{F}(\phi, \theta, t).$$

For $\phi \in (0, \pi)$ and $t \in (0, \infty)$, this function vanishes precisely when F does, and its Jacobian at $(\pi/2, \pi/4, t_0)$ is full rank if and only if the Jacobian of F is full rank. Also, we recall that the variable s is implicitly a function of ϕ, θ , and t , as determined by the equation

$$4e^{2i\theta} e^{i\phi} (s - e_1)(s - e_2) - t^2 (s - e_3) = 0$$

Step (1). In order to differentiate \hat{F} we establish the following notation:

$$\hat{F}(\phi, \theta, t) = t^2 B(s(\phi, \theta, t)) + 4e^{2i\phi} C(s(\phi, \theta, t))$$

$$B(s) = \int_0^1 \frac{\wp - e_3}{(\wp - s)(\wp - \bar{s}e^{-2i\phi})} dz$$

$$C(s) = \int_0^1 \frac{\prod(\bar{\wp} - \bar{e}_i)}{(\bar{\wp} - \bar{s})(\bar{\wp} - se^{2i\phi})} d\bar{z}$$

$$\operatorname{Re}(\hat{F}) = R = t^2 \operatorname{Re} B + 4 \cos 2\phi (\operatorname{Re} C) - 4 \sin 2\phi (\operatorname{Im} C)$$

$$\operatorname{Im}(\hat{F}) = I = t^2 \operatorname{Im} B + 4 \sin 2\phi (\operatorname{Re} C) + 4 \cos 2\phi (\operatorname{Im} C)$$

$$s(\phi, \theta, t) = u(\phi, \theta, t) + iv(\phi, \theta, t).$$

We now differentiate R and I and then evaluate these expressions at $p = (\phi_0, \theta_0, t_0, s_0) = (\pi/2, \pi/4, t_0, s_0)$.

Remark: The point p is written as though it is an element of \mathbb{R}^4 . This error is intentional as our expressions will involve s as well as the variables ϕ, θ , and t ; these expressions remain simpler if the relationship between s_0 and $(\pi/2, \pi/4, t_0)$ is suppressed.

Computations reveal that

$$\left. \frac{\partial R}{\partial t} \right|_p = 2t_0 B(s_0) + \frac{\partial u}{\partial t} \left(t_0^2 \frac{\partial B}{\partial u} - 4 \frac{\partial C}{\partial u} \right)$$

$$\left. \frac{\partial I}{\partial t} \right|_p = 0$$

$$\left. \frac{\partial R}{\partial \theta} \right|_p = 0$$

$$\left. \frac{\partial I}{\partial \theta} \right|_p = \frac{\partial v}{\partial \theta} \frac{1}{i} \left(t_0^2 \frac{\partial B}{\partial v} - 4 \frac{\partial C}{\partial v} \right).$$

The details for these equations are contained in Appendix A, as are the arguments that $R_t(p) > 0$ and $I_\theta(p) > 0$. Together we have $\det D\hat{F}_{(\theta,t)}(p) > 0$, completing the first step.

Step (2). To argue that $DF_{(\theta,t)}(p)$ has full rank at p we relate the (θ, t) Jacobians of F and \hat{F} :

$$\hat{F}(\phi, \theta, t) = |s - e_3|^{-1} \cdot F(\phi, \theta, t)$$

$$\begin{pmatrix} R_\theta & R_t \\ I_\theta & I_t \end{pmatrix} = \begin{pmatrix} |s - e_3|_\theta^{-1} \cdot \tilde{R} & |s - e_3|_t^{-1} \cdot \tilde{R} \\ |s - e_3|_\theta^{-1} \cdot \tilde{I} & |s - e_3|_t^{-1} \cdot \tilde{I} \end{pmatrix} + \frac{1}{|s - e_3|} \begin{pmatrix} \tilde{R}_\theta & \tilde{R}_t \\ \tilde{I}_\theta & \tilde{I}_t \end{pmatrix}$$

where $\tilde{R} = \text{Re}(F)$ and $\tilde{I} = \text{Im}(F)$. Evaluating these expressions at p , where $R = I = \tilde{R} = \tilde{I} = 0, e_3 = 0$, and $s = s_0$ yields

$$\begin{pmatrix} 0 & R_t \\ I_\theta & 0 \end{pmatrix} = \frac{1}{s_0} \begin{pmatrix} \tilde{R}_\theta & \tilde{R}_t \\ \tilde{I}_\theta & \tilde{I}_t \end{pmatrix}$$

As a result, the (θ, t) -Jacobian of $F(\phi, \theta, t)$ has full rank at p .

The implicit function theorem now implies that for ϕ near $\pi/2$ the parameters θ and t depend smoothly on ϕ and may be chosen so that $F(\phi, \theta(\phi), t(\phi)) = F(\phi) = 0$. This finishes our proof. q.e.d.

3.4. Additional Remarks. We note here that via a result of Montiel-Ros (see [17]) we can conclude that our initial surface $S(1, \pi/2)$ is non-degenerate and hence belongs to an analytic, one-dimensional family of minimal surfaces. To see this, we simply need to observe that the branch values of g lie along a great circle. Because the underlying torus is square, we obtain the following algebraic description:

$$\mathcal{R} = \left\{ (z, w) \in \hat{\mathbb{C}} \times \hat{\mathbb{C}} : w^2 = \frac{z^2 - a^2}{z^2 + a^2} \right\},$$

where $\pm a$ and $\pm ia$ are the branch values of the Guass map g . Hence, we need to show that $a = 1$ in order to conclude non-degeneracy.

When $\phi = \pi/2$ and hence $\theta = \pi/4$, it is straightforward to verify that the quadratic differential $(dg/g) dh$ is purely real along the vertical lines in the square torus that join ω_1 to ω_3 . This implies the presence of a planar reflection $(z, w) \mapsto (1/z, w)$, which, in turn, implies $a = 1$.

Unfortunately, the functions $\theta(\phi)$ and $t(\phi)$ are not easily analyzed, but symmetry governs their behavior under the transformation $\phi \mapsto (\pi - \phi)$.

Proposition 6. *If (ϕ, θ, t) vanishes under F , then so does the triple $(\pi - \phi, \pi/2 - \theta, t)$*

Proof. First, we establish that $s(\pi - \phi, \pi/2 - \theta, t) = \overline{s(\phi, \theta, t)}$. This follows from a straightforward analysis of the equation that defines s . Specifically,

$$\begin{aligned} 4e^{2i\theta} e^{i\phi} (s - e_1)(s - e_2) &= t^2(s - e_3) \\ 4e^{-2i\theta} e^{-i\phi} (\bar{s} - \bar{e}_1)(\bar{s} - \bar{e}_2) &= t^2(\bar{s} - \bar{e}_3) \end{aligned}$$

The second equation defines the function \bar{s} . Given any odd integer n , the change of parameters $\phi \mapsto \pi - \phi$ and $\theta \mapsto n\pi/2 - \theta$ imply that \bar{s} and s satisfy the same equation. To see this, we first note that the invariants $e_i(\phi)$ satisfy $e_i(\pi - \phi) = \bar{e}_i(\phi)$. We now substitute into the first equation, yielding

$$\begin{aligned} 4e^{2i(n\pi/2 - \theta)} e^{i(\pi - \phi)} (s - \bar{e}_1)(s - \bar{e}_2) &= t^2(s - \bar{e}_3) \\ \Rightarrow 4e^{-2i\theta} e^{-i\phi} (s - \bar{e}_1)(s - \bar{e}_2) &= t^2(s - \bar{e}_3) \\ \Rightarrow s(\pi - \phi, n\pi/2 - \theta, t) &= \bar{s}(\phi, \theta, t) \end{aligned}$$

However, since we choose $\theta \in (0, \pi/2)$, the only allowable value of n is $n = 1$. This establishes the desired property.

Now we claim that $\hat{F}(\phi, \theta, t) = \overline{\hat{F}(\pi - \phi, \pi/2 - \theta, t)}$, which finishes the proof. To see this, we show that it is true for the functions $B(\phi, \theta, t)$ and $C(\phi, \theta, t)$. Because the \wp function and its associated invariants e_i satisfy

$$\begin{aligned} \wp(z; \pi - \phi) &= \overline{\wp(\bar{z}; \phi)} \\ e_i(\pi - \phi) &= \bar{e}_i(\phi) \end{aligned}$$

under this transformation of variables, the function B becomes

$$\begin{aligned}
B(\pi - \phi, \pi/2 - \theta, t) &= \int_0^1 \frac{\wp(x; \pi - \phi) - e_3(\pi - \phi)}{(\wp(x; \pi - \phi) - s)(\wp(x; \pi - \phi) - \bar{s}e^{2i\phi})} dx \\
&= \int_0^1 \frac{\bar{\wp}(x; \phi) - \bar{e}_3(\phi)}{\bar{\wp}(x; \phi) - s)(\bar{\wp}(x; \phi) - \bar{s}e^{2i\phi})} dx
\end{aligned}$$

In the expression above, the parameter s now depends on $\pi - \phi$ and $\pi/2 - \theta$. We may replace the s terms above with \bar{s} , giving

$$\begin{aligned}
B(\pi - \phi, \pi/2 - \theta, t) &= \int_0^1 \overline{\left(\frac{\wp(x) - e_3}{(\wp(x) - s)(\wp(x) - \bar{s}e^{-2i\phi})} \right)} dx \\
&= \bar{B}(\phi, \theta, t)
\end{aligned}$$

An analogous computation with the function $C(\phi, \theta, t)$ gives

$$C(\pi - \phi, \pi/2 - \theta, t) = \bar{C}(\phi, \theta, t)$$

Finally, because $\hat{F} = t^2 B + 4e^{2i\phi} C$, we have

$$\hat{F}(\pi - \phi, \pi/2 - \theta, t) = t^2 \bar{B}(\phi, \theta, t) + 4e^{-2i\phi} \bar{C}(\phi, \theta, t) = \overline{\hat{F}(\phi, \theta, t)}$$

This completes the proof.

q.e.d.

Corollary 1. *For ϕ sufficiently close to $\pi/2$ the functions $\theta(\phi)$ and $t(\phi)$ satisfy*

$$\begin{aligned}
\theta(\pi - \phi) &= \pi/2 - \theta(\phi) \\
t^2(\pi - \phi) &= t^2(\phi).
\end{aligned}$$

Proof. This follows from Proposition 6 and Theorem 3.

q.e.d.

In other words, the function $\theta(\phi) - \pi/4$ is odd about the point $\phi = \pi/2$. Therefore, to demonstrate that the values of θ are changing as the torus parameter ϕ changes, we simply need to argue that $\theta(\phi)$ is non-constant.

One is tempted to show, for example, that it is impossible to solve the period problem on the hexagonal torus $\phi = \pi/3$ with $\theta = \pi/4$, but we have had no success in doing this. Similarly, a maximum principle at infinity (such as used in [16]) seems useful in demonstrating that $\theta = \pi/4 \Rightarrow \phi = \pi/2$, but, again, results in this direction have not yet been obtained.

However, it should be noted that based on observations of Weber-Hoffman-Wolf [25] regarding the uniqueness of the underlying torus upon which the singly periodic genus helicoid is based, it is likely $S(1, 2\theta)$ cannot be obtained by appropriately puncturing *any* rhombic torus. In particular, letting ϕ_0 denote the value of ϕ upon which $\mathcal{H}(1)$ is defined, it should follow that for all $\phi \notin (\pi - \phi_0, \phi_0)$ it is impossible to

puncture \mathbb{C}/Λ_ϕ in such a way to obtain $S(1, 2\theta)$. This leads to the following:

Conjecture 1. *For all $\theta \in (0, \pi/4]$, $S(1, 2\theta) \cong \mathbb{C}/\Lambda_\phi - \{a_1, a_2, a_3, a_4\} \Rightarrow \phi \in (\pi - \phi_0, \phi_0)$.*

4. The Analytic Solution Curve and Flat Structures

In this section we obtain useful gdh and $(1/g)dh$ flat structure representations for the surfaces $S(1, 2\theta)$; these structures are parameterized by a triple (ℓ, θ, α) . We first observe that the period condition $\hat{F}(\phi, \theta, t) = 0$ determines an analytic curve in (ϕ, θ, t) -space. From this we conclude that the surfaces $S(1, 2\theta)$ exist until one (or more) of the parameters (ϕ, θ, t) degenerates. As a consequence, associated gdh and $(1/g)dh$ flat structures exist until one (or more) of the parameters (ℓ, θ, α) degenerates.

4.1. The Analytic Curve. The function $\hat{F}(\phi, \theta, t) = R(\phi, \theta, t) + iI(\phi, \theta, t)$ is analytic in ϕ, θ , and t for $(\phi, \theta, t) \in \mathcal{P}$. This follows from the definition of \hat{F} :

$$t^2 \int_0^1 \frac{\wp - e_3}{(\wp - s)(\wp - e^{-2i\phi}\bar{s})} dx + 4e^{2i\phi} \int_0^1 \frac{\prod(\bar{\wp} - \bar{e}_i)}{(\bar{\wp} - \bar{s})(\bar{\wp} - se^{2i\phi})} dx$$

For non-degenerate values of ϕ , the Weierstrass \wp function $\wp(z; \tau)$ is analytic in both z and $\tau = e^{i\phi}$, and hence so are the values $e_i = \wp(\omega_i; \tau)$. Clearly the functions t^2 and $e^{2i\phi}$ depend analytically on t and ϕ , respectively. The only other parameter we need to check is $s = s(\phi, \theta, t)$.

Proposition 7. *The function $s(\phi, \theta, t)$ is analytic on \mathcal{P}*

Proof. The proof is contained in Appendix B. q.e.d.

We can now conclude that the functions $R(\phi, \theta, t)$ and $I(\phi, \theta, t)$ are analytic in \mathcal{P} . Moreover, the solution curve determined by $R = I = 0$ necessarily contains an analytic arc passing through the point $(\pi/2, \pi/4, t_0)$. We have already established that near this point, θ and t are functions of ϕ . As a result, the solution curve cannot be branched at $(\pi/2, \pi/4, t_0)$.

Using Sullivan's Local Euler Characteristic Theorem (see [9]), we know that this solution curve must be extendable. Moreover, because of the uniqueness result from Theorem 2, it is therefore impossible for this solution curve to "close up" within the slab \mathcal{P} , as this would force a branching at $(\pi/2, \pi/4, t_0)$.

We are forced to conclude that the solution curve necessarily intersects $\partial P = \{(\phi, \theta, t) : \phi \in \{0, \pi\} \text{ or } t \in \{0, \infty\} \text{ or } \theta \in \{0, \pi/2\}\}$. Even if the curve branches at certain points, again by [9] there is always at least one path that persists. Unfortunately, the possible limit points in ∂P are difficult to identify since the parameters (ϕ, θ, t) are not well adapted to detect when the period condition fails; in particular, it is difficult to

demonstrate that $R \neq 0$ or $I \neq 0$ when, say, the parameter $\phi \rightarrow 0, \pi$. It is possible to restrict one particular degeneration, though.

Remark: Let $x \in [a, b]$ with a and b possibly infinite. Here and for the remainder of the paper x^* will denote an interior value of the real variable x , e.g. $\phi^* \in (0, \pi)$. We will say that the variable x does **not degenerate** if $x \rightarrow x^*$, and we will say that x does **degenerate** otherwise.

Proposition 8. *The period problem becomes impossible to solve as $(\phi, \theta, t) \rightarrow (\phi^*, \theta, \infty)$ or $(\phi, \theta, t) \rightarrow (\phi^*, \theta, 0)$.*

Proof. This follows from examining the period function $\hat{F}(\phi, \theta, t)$, which is given by

$$t^2 \int_0^1 \frac{\wp - e_3}{(\wp - s)(\wp - e^{-2i\phi}\bar{s})} dx + 4e^{2i\phi} \int_0^1 \frac{\prod(\bar{\wp} - \bar{e}_i)}{(\bar{\wp} - \bar{s})(\bar{\wp} - se^{2i\phi})} dx$$

Observe that the parameter θ appears implicitly, as a variable upon which s depends. The integrands remain bounded since ϕ does not degenerate, and if $t \rightarrow 0$ then $s \rightarrow e_1$ or $s \rightarrow e_2$, and as we have already noted, at these values $\hat{F} = e^{2i\phi}$. Similarly, as $t \rightarrow \infty, s \rightarrow e_3$ where $\hat{F} = \infty$. In either case, $\hat{F} \neq 0$ and so the period problem is unsolved. q.e.d.

We would like to argue that if ϕ degenerates, then the period problem fails, but this is difficult to do. Instead, we assume that the period problem is solved and thereby obtain flat structures that are parameterized by new coordinates, (ℓ, θ, α) where $\ell \in (0, \infty)$ and $\alpha \in (0, \pi/2)$. Certain degenerations of these geometric coordinates yield contradictions, while other degenerations will imply that ϕ cannot degenerate.

4.2. Flat Structures. As described in [27], a one-form η on a Riemann surface \mathcal{R} gives rise to a cone metric. In particular, if z is a local coordinate on \mathcal{R} , then one can use $\eta = f(z)dz$ to define a line element ds_η by

$$ds_\eta = |\eta| = |f(z)||dz|$$

Away from the zeroes and poles of η , the metric ds_η has curvature

$$K = -\frac{2}{f(z)} \partial \bar{\partial} \log f(z) = 0$$

since f is meromorphic.

At a zero or pole p of η , we have $\eta = (z^k + \text{higher-order terms})dz$, and so ds_η is isometric to a Euclidean cone metric with cone angle $2\pi(k+1)$ at p . In particular, because ds_η is a cone metric of non-positive curvature, unique geodesics in a given homotopy class are guaranteed to exist, provided the curves do not pass through a pole or zero of η (see [22] for more details).

The developing map $D : \mathcal{R} \rightarrow \mathcal{R}'$ given by

$$D(z) = \int^z \eta$$

takes η -geodesics in \mathcal{R} to straight lines, and is conformal except at the finitely many points where η has a zero. Akin to Riemann's original constructions, the surface \mathcal{R}' is built so that $D(z)$ has a well defined inverse; the important distinction is that \mathcal{R}' is obtained as a polygonal domain in \mathbb{C} with identifications. This is accomplished by developing enough η -geodesics in \mathcal{R} ; these representations are called the flat structure representations of η .

For minimal surfaces, the one-forms gdh and $(1/g)dh$ underly useful cone metrics $|gdh|$ and $|(1/g)dh|$, respectively. Recall that the horizontal period condition is given by

$$\int_{\gamma} gdh = \overline{\int_{\gamma} \frac{1}{g} dh}.$$

This condition is satisfied provided that the gdh -geodesic and the $(1/g)dh$ -geodesic belonging to the homology class of γ develop into conjugate line segments. Hence, the horizontal period condition can easily be built into the flat structure representations for gdh and $(1/g)dh$.

Conversely, one can start with proposed gdh and $(1/g)dh$ flat structures, constructed so that the horizontal period problem is solved, and typically represented as polygons with various edges identified. These flat structures will determine *some* compact Riemann surface with punctures, but it is not clear that they will determine the same one.

The (horizontal) period problem is in this manner replaced by a question of conformal type. Even with the period problem restricting the possible gdh and $(1/g)dh$ flat structures, there are often a number of free parameters left undetermined (typically the lengths of the polygon's edges). One is then required to demonstrate that for some choice of these parameters, enough conformal invariants agree, ensuring that the pair of flat structures represent one-forms defined on the same underlying Riemann surface.

After accomplishing this, one then has to verify that the vertical period problem is solved, but this is often accomplished by making use of the fact that

$$dh = \sqrt{(gdh) \left(\frac{1}{g} dh \right)}.$$

Moreover, the entire procedure is facilitated by the presence of symmetry within the Riemann surface \mathcal{R} , for lines of symmetry on \mathcal{R} are necessarily η -geodesics.

4.2.1. The Helicoid “on its side”. Here is a straightforward and helpful example of a minimal surface’s flat structure representation: the helicoid “on its side.” To develop a convenient gdh flat structure for this minimal surface, observe that the gdh and $(1/g)dh$ flat structures for any surface agree with the gdh and $(1/g)dh$ flat structures for its conjugate surface, up to rotation (see, for example, [24]). Hence, we can use a catenoid on its side to develop the gdh flat structure for a helicoid on its side (see Figure 3 below).

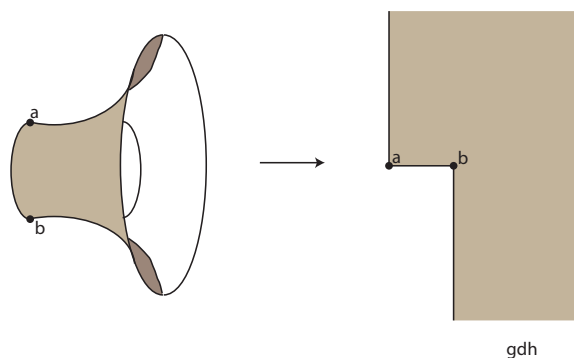


Figure 3. gdh flat structure for the helicoid “on its side”

The corresponding $(1/g)dh$ flat structure looks exactly the same, only the points a and b are relabeled $a \leftrightarrow b$.

4.2.2. The Scherk-Karcher Surface $S(1, \pi/2)$. Here is another illustrative example, one that also has relevance to our problem. Let $\mathcal{R} = \mathbb{C}/\Lambda_{\pi/2} - \{a_1, a_2, a_3, a_4\}$ be our punctured square torus corresponding to the triple $(\phi, \theta, t) = (\pi/2, \pi/4, t_0)$. As we have already noted, the punctures a_i are required to lie along the lines of symmetry as depicted in Figure 4, where the divisor data for gdh and $(1/g)dh$ is also depicted. Again, because lines of symmetry are geodesics for both cone metrics $|gdh|$ and $|(1/g)dh|$, we develop the flat structures depicted in Figure 5.

Observe that the period problem is solved if and only if the gdh -geodesic and $(1/g)dh$ -geodesic belonging to the homology class of the line segment joining 0 and $1/2$ (and, by reflection, those joining the other half-period points) develop into conjugate line segments of the same length ℓ .

The only free parameter in these flat structures is this length ℓ . In this problem, it is sufficient to consider one conformal invariant, namely the Extremal Length of a particular set of curves. On the gdh flat structure, the Extremal Length is given by one value, and on the $(1/g)dh$ flat structure it is given by another, possibly different, value. We will review

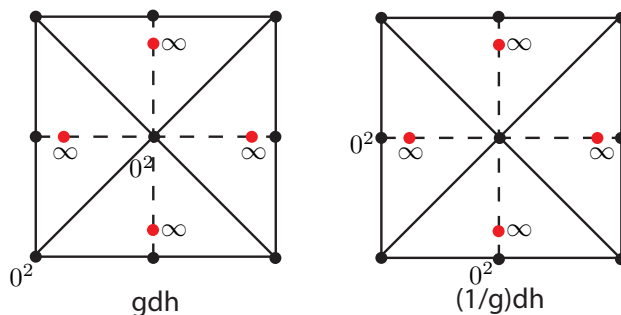


Figure 4. gdh and $(1/g)dh$ divisor data for $S(1, \pi/2)$

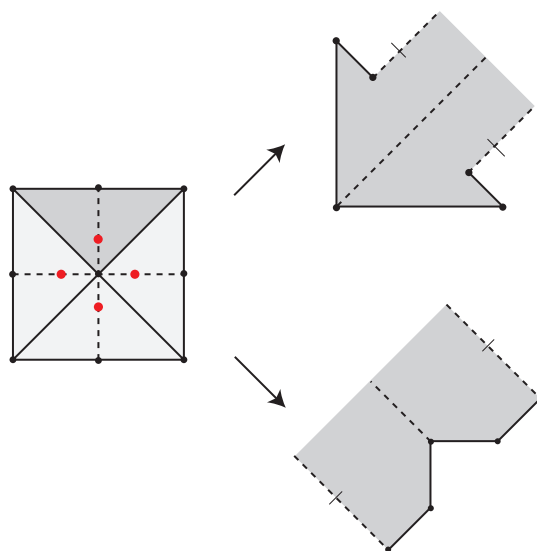


Figure 5. gdh and $(1/g)dh$ flat structures for $S(1, \pi/2)$

the notion of Extremal Length in the next section, but, as proven in [26], there is a finite choice of ℓ for which these two values agree. Moreover, as with our uniqueness result concerning the square torus, there is only one such value of ℓ for which this happens.

4.3. Remarks on the Developing Map and Teichmüller Space. In their constructions, [27], Weber-Wolf typically assumed a maximum amount of symmetry. As a result, the flat structure representations for

gdh and $(1/g)dh$ likewise enjoy a great deal of symmetry. So much so, in fact, that these structures can often be “folded” down to simply connected regions bounded by line segments and rays that meet at 90° and 270° ; such domains are called **orthodisks**.

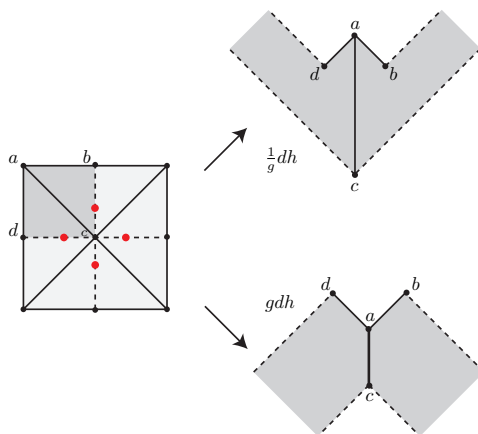


Figure 6. Orthodisk flat structures for $S(1, \pi/2)$

When working with orthodisks, the gdh and $(1/g)dh$ geodesics that join various 0s, poles, and regular points often overlap, and, as a result, the conformal map that necessarily exists between the gdh and $(1/g)dh$ flat structures is forced to be *edge-preserving*. As a result, the flat structures are not merely conformally equivalent but Teichmüller equivalent (see [1] or [18] for more details about this notion).

Figure 5 depicts non-simply connected flat structure representations for gdh and $(1/g)dh$. However, orthodisks *are* available in this setting; they are obtained by developing the region indicated in Figure 6.

Orthodisks will *not* be available for the surfaces $S(1, 2\theta)$. This follows because symmetry is necessarily destroyed by moving away from the square torus. Hence, the gdh and $(1/g)dh$ flat structures that we will develop will *only* be conformally equivalent, not Teichmüller equivalent, as they are obtained from Riemann surfaces that have been slit differently.

4.4. The $(1/g)dh$ Flat Structure for $S(1, 2\theta)$. For minimal surfaces $S(1, 2\theta)$ near the Scherk-Karcher surface $S(1, \pi/2)$, we obtain $(1/g)dh$ -flat structures such as the ones depicted in Figure 7.

The figure depicts one quarter of the $(1/g)dh$ flat structure, developed from the quarter of the underlying rhombic torus depicted on the left. The paths joining various half-period points, as well as paths joining

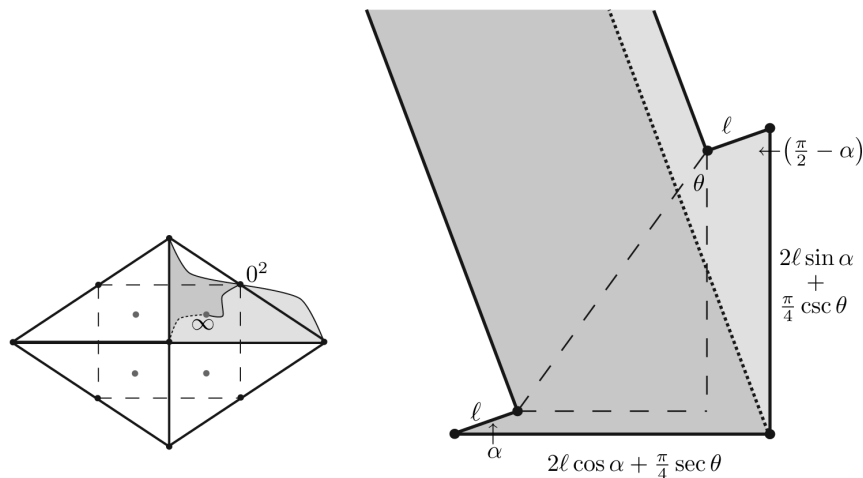


Figure 7. $(1/g)dh$ flat structure for $S(1, 2\theta)$

half-period points to the puncture (the solid and dotted paths, respectively), are $(1/g)dh$ -geodesics and so they develop to (correspondingly solid and dotted) straight line segments.

Observe that the horizontal and vertical lines of symmetry develop to vertical and horizontal lines of symmetry. Also note that the geodesic joining ω_1 to the puncture a_1 is chosen to meet the other two geodesics (the solid paths) at 90° . This geodesic develops into a ray, and in the flat structure representation shown above, it is depicted as two, identified rays; the identification is obtained via the translation $\vec{v} \mapsto 2\pi i \cdot \text{Res}_{a_1}(gdh) + \vec{v}$. The length of this translation vector is $\pi/4 \sec \theta \csc \theta$ and is the hypotenuse of the dotted triangle depicted above.

The complete $(1/g)dh$ flat structure is obtained by reflecting the depicted quarter across the orthogonal lines of symmetry, and then making appropriate identifications between the edges labeled with length ℓ .

We also remark here that the value α must lie in $(0, \pi/2)$. If $\alpha = 0$, for example, then the geodesic joining the half-period points ω_1 and ω_2 would coincide with the geodesic joining ω_1 to ω_3 , which is a line of symmetry in the torus and the flat structure. While it is possible for the intersection of two cone-metric geodesics to contain more than a single point, this can only happen if one of these geodesics approaches a zero or a pole of the cone-metric. Since this is *not* the case with our $|(1/g)dh|$ cone-metric and either line of symmetry, we conclude that α cannot equal 0 or $\pi/2$.

Additionally, neither of the edges marked with an ℓ can intersect a line of symmetry, since if this were to happen the hypotenuse of the dotted

triangle would have to vanish, which is impossible since this value is, again, given by $\pi/4 \sec \theta \csc \theta$.

In summary, $(1/g)dh$ flat structures are parameterized by a triple $(\ell, \theta, \alpha) \in (0, \infty) \times (0, \pi/2) \times (0, \pi/2)$, and possess quarters that we may represent via diagrams such as the one given in Figure 7.

4.5. The gdh Flat Structure for $S(1, 2\theta)$. If we similarly depict the gdh -geodesics joining the half-period points and the puncture, we develop the flat structure representation depicted in Figure 8, which corresponds to a quarter of the underlying rhombic torus.

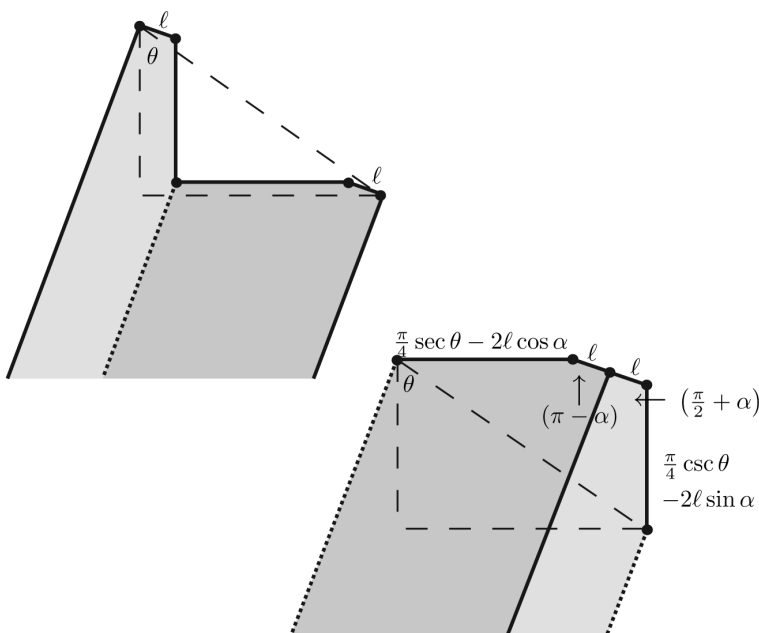


Figure 8. gdh flat structure for $S(1, 2\theta)$

We have presented two flat structure representations for the gdh flat structure. The second one is obtained from the first by cutting along the dotted geodesic, and then gluing along the identified, solid geodesic(s). In the top picture, the solid lines are identified, and in the bottom picture the dotted lines are identified. The complete flat structure is similarly recovered by reflecting across the horizontal and vertical line segments and making appropriate identifications.

Again, the straight line segments of length ℓ in Figure 8 are the developed gdh -geodesics that belong to the same homology class as the Euclidean line segments joining various half-period points along the perimeter of the rhombus that represents our torus (on the square torus, these geodesics coincide with the Euclidean line segments).

We remark that, a priori, it is possible for the gdh -geodesics joining two half-period points to coincide with a line of symmetry; this possibility exists because the two lines of symmetry cross the double-zeroes of the form gdh . However, because the gdh flat structure and the $(1/g)dh$ flat structure enjoy a conjugacy relationship corresponding to a solved period problem, the angles between the lines of symmetry and such geodesics are necessarily given by the values indicated above, namely $\pi - \alpha$ and $\pi/2 + \alpha$. If these geodesics were to coincide for some surface $S(1, 2\theta)$, then we would have $\alpha = \pi$ or $\alpha = -\pi/2$, but, as previously noted, the parameter α can only take values in $(0, \pi/2)$.

In summary, quarters of the gdh flat structures are represented by diagrams such as the ones in Figure 8, and are parameterized by the same triple (ℓ, θ, α) used to parameterize $(1/g)dh$ flat structures.

4.6. A Bit More About Both Structures. The flat structures feature three undetermined parameters: ℓ , θ , and α . Observe that a non-degenerate triple of these geometric coordinates (ℓ, θ, α) corresponds to a non-degenerate triple of our original coordinates (ϕ, θ, t) . We also record the following relationships between ℓ and the underlying 1-forms:

$$(3) \quad 2\ell = 2 \int_{\gamma_+} |gdh| = \left| \int_0^1 gdh \right|$$

$$(4) \quad = 2 \int_{\gamma_-} \left| \frac{1}{g} dh \right| = \left| \int_0^1 \frac{1}{g} dh \right|$$

where γ_+ and γ_- denote the respective gdh - and $(1/g)dh$ -geodesics homologous to the line segment $[0, 1/2]$.

The gdh flat structure also reveals key relationships between the parameters ℓ , θ , and α . Specifically,

$$(5) \quad \frac{\pi}{4} \sec \theta - 2\ell \cos \alpha > 0$$

$$(6) \quad \frac{\pi}{4} \csc \theta - 2\ell \sin \alpha > 0$$

From these inequalities we find

$$(7) \quad \ell \rightarrow \infty \iff \theta \rightarrow 0 \text{ and } \alpha \rightarrow \pi/2$$

or

$$(8) \quad \ell \rightarrow \infty \iff \theta \rightarrow \pi/2 \text{ and } \alpha \rightarrow 0$$

In particular, if the parameter ℓ degenerates to ∞ , then the parameter θ degenerates as well, which will imply that $S(1, 2\theta)$ exists for every $\theta \in (0, \pi/2)$.

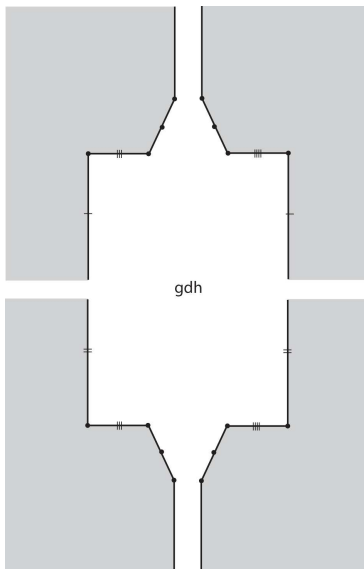


Figure 9. gdh flat structure for $\mathcal{H}(1)$ “on its side”

4.7. The gdh Flat Structure for $\mathcal{H}(1)$. Finally, because we claim that our surfaces limit on the singly periodic, genus-one helicoid (on its side), we include here the gdh flat structure for this surface.

Again, similarly indicated edges are identified, and note the relationship with or similarity to the gdh flat structure for the genus zero helicoid on its side. Indeed, the presence of this “added corner” (as well as the helicoidal ends) confirms, at least morally or intuitively, that this is an accurate depiction of gdh for $\mathcal{H}(1)$.

We will be able to make this conclusion more precise by analyzing the form gdh that gives rise to this flat structure. One way to accomplish this is to develop the gdh flat structure for the singly periodic, genus one helicoid (on its side); indeed, this form will necessarily have divisor data (double zeroes and double poles) that give rise to Figure 9.

In the next section we will obtain the Figure 9 as a limit of gdh flat structures for the surfaces $S(1, 2\theta)$. As a result, the form gdh (as well as $(1/g)dh$) can be understood in terms of the parameters (ϕ, θ, t) . A straightforward residue calculation and the presence of symmetry will allow us to use a result from [3] and conclude that the corresponding minimal surface is the singly periodic genus one helicoid $\mathcal{H}(1)$.

5. Taking a Limit

In this section we use various extremal lengths to demonstrate that certain degenerations of our surfaces are impossible. As a result of Theorem 3, we know that perturbed gdh and $(1/g)dh$ flat structures exist

and remain conformally equivalent. Our goal is to show that the gdh flat structures degenerate to the gdh flat structure for the singly periodic genus-one helicoid. This will be accomplished by demonstrating that all other possible degenerations violate either the conformal equivalence between the $(1/g)dh$ and gdh flat structures or the period condition. We outline the main steps for this procedure below.

Step (1). We show that θ must degenerate. To accomplish this, we first prove Lemma 1, which asserts $\ell \rightarrow 0 \Rightarrow \phi \rightarrow \phi^*$. Lemma 2 makes use of the bilinear relation applied to $gdh \wedge dz$ and $(1/g)dh \wedge dz$, as well as Lemma 1, to establish that $\ell \rightarrow 0 \Rightarrow \theta \rightarrow 0$ (or $\pi/2$). Finally, Lemma 3 uses Extremal Length arguments to conclude that limit triples of the form $(\ell^*, \theta^*, 0)$ and $(\ell^*, \theta^*, \pi/2)$ are impossible. Theorem 4 collects these results to conclude that the parameter θ necessarily degenerates. As a consequence, we learn that for every $\theta \in (0, \pi/2)$, the surface $S(1, 2\theta)$ exists as an immersed surface in \mathbb{R}^3 .

Step (2). We show that ℓ degenerates if and only if the torus parameter ϕ does *not* degenerate and the quantity $|\operatorname{Im}(se^{i\phi})| \csc \theta \sec \theta$ degenerates to 0 or ∞ . This is the content of Lemmas 4 and 5, which make use of various curve systems and their corresponding extremal lengths.

Step (3). We next argue that the quantity $|\operatorname{Im}(se^{i\phi})| \csc \theta \sec \theta$ cannot tend to 0 or ∞ , and so the parameter ℓ cannot degenerate. This is the content of Lemma 6. (The “doubling technique” defined in Rosenberg-Toubiana [20] and used in Meeks-Rosenberg [15] for doubly periodic surfaces can be used to this end, too.) As a result, few limiting flat structures are available as possibilities, and, using Extremal Length arguments, all but one yield contradictions. We then show that this remaining flat structure agrees with that of the gdh flat structure for $\mathcal{H}(1)$, completing the proof of Theorem 5.

First, though, we review the notion of extremal length in general as well as in the particular case of a (punctured) rhombic torus.

5.1. Extremal Length. There are a number of ways to define Extremal Length. Let Γ be a set of (rectifiable) curves on a Riemann surface \mathcal{R} , and let $\mathcal{M} = \{\rho \geq 0\}$ denote the set of Borel measurable, conformal metrics on \mathcal{R} with finite area. The **extremal length** of Γ on \mathcal{R} is given by

$$\operatorname{Ext}_{\mathcal{R}}(\Gamma) = \sup_{\rho \in \mathcal{M}} \frac{\inf_{\gamma \in \Gamma} (L_{\rho}(\gamma))^2}{A_{\rho}(\mathcal{R})}$$

where $L_{\rho}(\gamma)$ denotes the ρ -length of the curve γ , and $A_{\rho}(\mathcal{R})$ denotes the ρ -area of \mathcal{R} .

5.1.1. Basic Properties. If $f : \mathcal{R} \rightarrow \mathcal{R}'$ is a conformal map, then $\operatorname{Ext}_{\mathcal{R}}(\Gamma) = \operatorname{Ext}_{\mathcal{R}'}(f(\Gamma))$. As a result, it provides a notion of length that depends only on the underlying Riemann surface \mathcal{R} . The Extremal

Length of a set of curves enjoys a number of properties (see [2] for more details), but we mention only a few basic ones here. First, if $\Gamma' \subset \Gamma$ then $\text{Ext}(\Gamma') \geq \text{Ext}(\Gamma)$; in other words, one can obtain upper bounds by restricting the set of curves under consideration. Second, one can obtain lower bounds by equipping \mathcal{R} with a particular metric ρ_0 . That is

$$\text{Ext}_{\mathcal{R}}(\Gamma) \geq \frac{\inf_{\gamma \in \Gamma} (L_{\rho_0}(\gamma)^2)}{A_{\rho_0}(\mathcal{R})}$$

There is another convenient way to obtain lower bounds. If every $\gamma \in \Gamma$ contains a sub-curve $\beta \in \mathcal{B}$, then $\text{Ext}_{\mathcal{R}}(\Gamma) \geq \text{Ext}_{\mathcal{R}}(\mathcal{B})$.

5.1.2. Extremal Length On A Torus. Often times Γ will consist of a homology class of curves. Let $\Gamma = [\gamma]$ be the homology class of a generator for the first homology group of a torus $\mathbb{C}/\{\omega_1, \omega_2\}$. The Extremal Length of Γ is well understood, even if the lattice degenerates.

Using the Euclidean metric on our rhombic tori $\mathcal{R} = \mathbb{C}/\Lambda_\phi$, one finds

$$\text{Ext}_{\mathcal{R}}(\Gamma) \geq \frac{1}{2 \cos(\phi/2) \sin(\phi/2)}$$

where, again, Γ denotes the homology class of either standard generator of $H_1(\mathcal{R})$. Similarly, let D_1 denote the diagonal of our torus that joins the origin to the point $1 + e^{i\phi}$, and let Γ_1 denote the homology class of D_1 . Then, again by using the Euclidean metric, we find

$$\text{Ext}_{\mathcal{R}}(\Gamma_1) \geq \frac{4 \cos^2(\phi/2)}{2 \cos(\phi/2) \sin(\phi/2)} = 2 \cot(\phi/2)$$

On the other hand, if we restrict Γ_1 to a subset of curves that are required to join the opposite sides of a rectangle with length $2 \cos(\phi/2)$ and width $(1/2) \sin(\phi/2)$, as in Figure 10, one obtains the following upper bound:

$$\text{Ext}_{\mathcal{R}}(\Gamma_1) \leq 4 \cot(\phi/2).$$

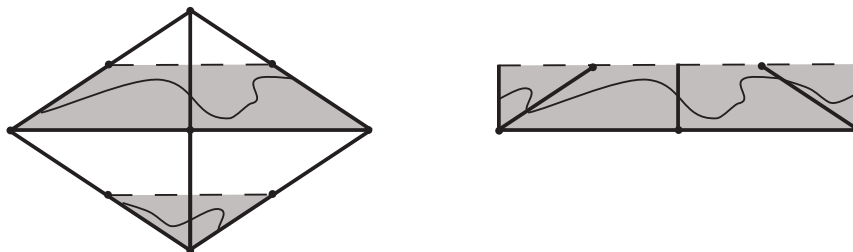


Figure 10. Γ_1 restricted to gray rectangle

We apply similar reasoning for the homology class Γ_2 of the other diagonal D_2 , and collect the resulting estimates here:

$$(9) \quad 4 \cot(\phi/2) \geq \text{Ext}_{\mathcal{R}}(\Gamma_1) \geq 2 \cot(\phi/2)$$

$$(10) \quad 4 \tan(\phi/2) \geq \text{Ext}_{\mathcal{R}}(\Gamma_2) \geq 2 \tan(\phi/2).$$

5.2. Some Notation and Sets of Curves. Many of the following Lemmas will make use of the same curve systems and surfaces, and so we establish notation that will be repeatedly used. While all of the families of curves used are homology classes, we remind the reader that the notion of extremal length is well defined for a mere *set* of curves. Indeed, we will restrict or enlarge these classes to sets whose extremal lengths are more readily approximated; this allows us to obtain lower and upper bounds, respectively.

$$\mathcal{R} = \mathbb{C}/\Lambda_\phi - \{a_1, a_2, a_3, a_4\}$$

$$\overline{\mathcal{R}} = \mathbb{C}/\Lambda_\phi$$

$$\Gamma = [\gamma] = \text{Homology Class of a Standard Generator for } H^1(\mathcal{R})$$

$$\Gamma_1 = [D_1] = \{\text{Homology Class of diagonal } D_1 \text{ joining } 0 \text{ to } 1 + e^{i\phi}\}$$

$$\Gamma_2 = [D_2] = \{\text{Homology Class of diagonal } D_2 \text{ joining } e^{i\phi} \text{ to } 1\}$$

$$\tilde{\Gamma} = \{\text{Homology Class of curves enclosing the punctures } a_1 \text{ and } a_2\}$$

$$\hat{\Gamma} = \{\text{Homology Class of curves enclosing the points } 1/2 + e^{i\phi}, a_1, a_2, \text{ and } 1 + e^{i\phi}/2 \text{ that only intersect the half of } D_1, \text{ as indicated in Figure 12}\}$$

$$\Gamma^* = \{\text{Homology Class of curves enclosing } a_1 \text{ and } a_3, \text{ that enclose no other punctures or half-period points, and that do not intersect either diagonal}\}$$

$$\text{Ext}_+(\cdot) = \text{Extremal Length on } gdh \text{ flat structure}$$

$$\text{Ext}_-(\cdot) = \text{Extremal Length on } (1/g)dh \text{ flat structure}$$

$$\text{Ext}_0(\cdot) = \text{Ext}_{\mathcal{R}}(\cdot)$$

$$\text{Ext}_{\overline{0}}(\cdot) = \text{Ext}_{\overline{\mathcal{R}}}(\cdot)$$

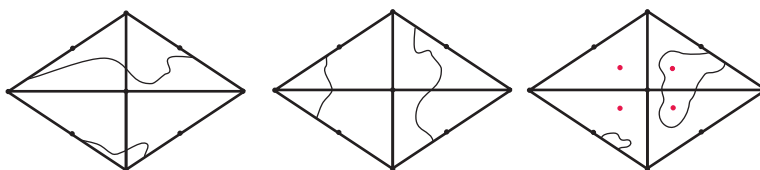


Figure 11. Curves in Γ_1, Γ_2 , and $\tilde{\Gamma}$, respectively

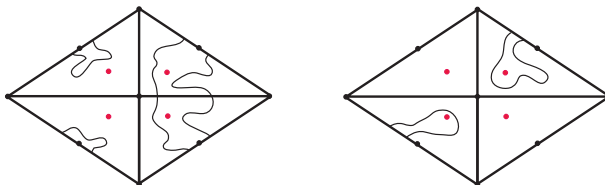


Figure 12. Curves in $\hat{\Gamma}$ and Γ^*

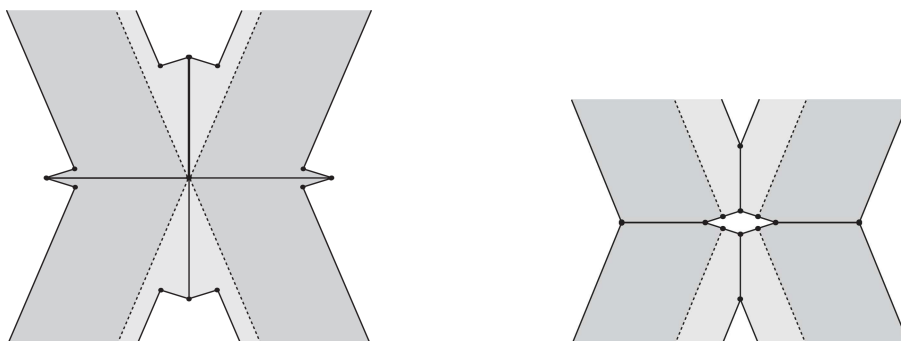


Figure 13. Complete $(1/g)dh$ (left) and gdh (right) flat structures

Because the gdh and $(1/g)dh$ flat structures are conformally equivalent to the punctured rhombic torus \mathcal{R} , we have $\text{Ext}_+(\mathcal{F}) = \text{Ext}_-(\mathcal{F}) = \text{Ext}_0(\mathcal{F})$ for any family \mathcal{F} of curves.

We will also make use of the entire gdh and $(1/g)dh$ flat structures, as opposed to quarters. This is necessary since for general $S(1, 2\theta)$, previously depicted quarters of these flat structures are *not* conformally equivalent. Indeed, these quarters were obtained by developing gdh and $(1/g)dh$ geodesics which may not, in general, agree. The complete flat structures are depicted in Figure 13.

5.3. Step 1: Proving θ Degenerates.

Lemma 1. *If $\ell \rightarrow 0$, then the torus parameter ϕ cannot degenerate.*

Proof. For a contradiction, suppose $\ell \rightarrow 0$ and that ϕ tends to 0 or π . Let $\Gamma'_i \subset \Gamma_i$ be the subset of the homology class of either standard generator for $H_1(\overline{\mathcal{R}})$ of our (non-punctured) torus, where Γ'_i is given by curves on the gdh flat structure such as the one depicted in Figure 14. These curves are not allowed to touch any edges other than the ones indicated; in other words, we have used the 1-form gdh to restrict the sets Γ_i .

The structure in Figure 14 has been rescaled by $1/\ell$, keeping the lengths of the identified edges fixed at 1 but causing the lengths of the horizontal and vertical lines of symmetry to become infinite. The second picture assumes that the parameter α degenerates, too, though whether

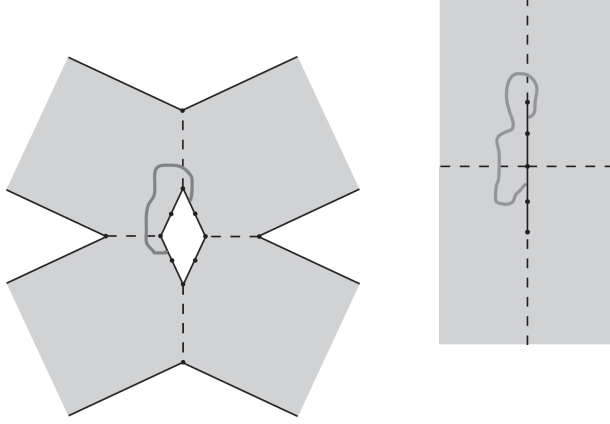


Figure 14. $\text{Ext}_+(\Gamma'_i) < \infty$ as $(\ell, \theta, \alpha) \rightarrow (0, \theta, \alpha)$

or not this additional degeneration takes place has no effect on our conclusion, namely, that as $\ell \rightarrow 0$ we have

$$\infty > \text{Ext}_+(\Gamma'_i) \geq \text{Ext}_+(\Gamma_i) = \text{Ext}_0(\Gamma_i).$$

However, if the parameter ϕ degenerates, then, $\text{Ext}_0(\Gamma_i) \rightarrow \infty$. Because the homology class of Γ_i on the punctured torus \mathcal{R} is contained in the homology class of Γ_i on the torus $\overline{\mathcal{R}}$ we have

$$\text{Ext}_0(\Gamma_i) \geq \text{Ext}_{\bar{0}}(\Gamma_i) \rightarrow \infty$$

producing the desired contradiction.

q.e.d.

Lemma 2. *It is impossible for (ℓ, θ, α) to limit on $(0, \theta^*, \alpha)$*

Proof. First, the bilinear relation applied to $gdh \wedge dz$ and $(1/g)dh \wedge dz$ combined with the period condition $\int gdh = \overline{\int (1/g)dh}$ yield

$$\begin{aligned} -2\ell \left(e^{-i\alpha} + e^{i\phi} e^{i\alpha} \right) &= \frac{\pi i}{4 \sin \theta \cos \theta} \left(e^{i\theta} (a_1 - a_3) - e^{-i\theta} (a_2 - a_4) \right) \\ -2\ell \left(e^{i\alpha} + e^{i\phi} e^{-i\alpha} \right) &= \frac{\pi i}{4 \sin \theta \cos \theta} \left(e^{-i\theta} (a_1 - a_3) - e^{i\theta} (a_2 - a_4) \right) \end{aligned}$$

Assuming $\ell \rightarrow 0$, we know from Lemma 1 that ϕ is not degenerating. Moreover, using that $a_2 = e^{i\phi} \overline{a_1}$ and $a_4 = e^{i\phi} \overline{a_3}$, the two equations above become

$$(11) \quad 0 = 2e^{i\phi/2} \cdot \text{Im} \left(e^{i\theta} e^{-i\phi/2} (a_1 - a_3) \right)$$

$$(12) \quad 0 = 2e^{i\phi/2} \cdot \text{Im} \left(e^{-i\theta} e^{-i\phi/2} (a_1 - a_3) \right)$$

In particular, we see that $(a_1 - a_3) \in (e^{-i\theta} e^{i\phi/2}) \mathbb{R} \cap (e^{i\theta} e^{i\phi/2}) \mathbb{R}$. As we are not allowing θ to limit on 0 or $\pi/2$, this implies that $(a_1 - a_3) = 0$ or ∞ . As it is impossible for our punctures to tend to ∞ , we are forced to conclude that $a_1 = a_3$ which implies $a_1 = \omega_3$. Hence, $\wp(a_1) = s \rightarrow e_3$ as $\ell \rightarrow 0$, which implies that $t \rightarrow 0$ and, via Proposition 8 and Lemma 1, this implies that the period problem is unsolved for arbitrarily small values of $\ell \Rightarrow \Leftarrow$. q.e.d.

Lemma 3. *It is impossible for (ℓ, θ, α) to limit on $(\ell^*, \theta^*, 0)$ or $(\ell^*, \theta^*, \pi/2)$*

Proof. Without loss of generality, it suffices to show only one of these triples is impossible. This follows because if the triple (ϕ, θ, t) corresponds to the flat-structure triple (ℓ, θ, α) , then the triple $(\pi - \phi, \pi/2 - \theta, t)$ corresponds to $(\ell, \pi/2 - \theta, \pi/2 - \alpha)$. Therefore, we will show that $(\ell^*, \theta^*, 0)$ is impossible.

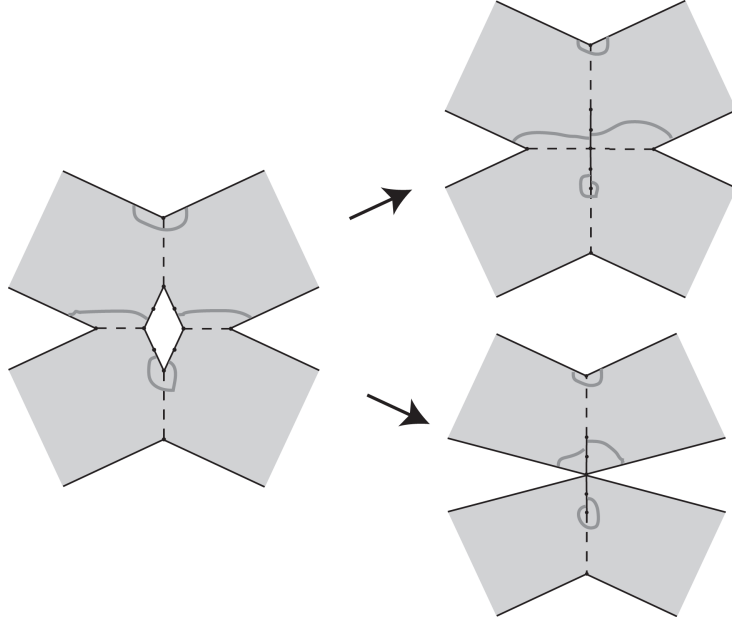


Figure 15. The set of curves Γ'_2 and its possible degenerations

In this case, the length of the vertical line segments present in the *gdh* flat structure tend to $(\pi/4) \csc \theta - 2\ell \sin \alpha \rightarrow (\pi/4) \csc \theta^* > 0$, while the horizontal lengths may or may not vanish, depending on the limiting behavior of $(\pi/4) \sec \theta - 2\ell \cos \alpha \rightarrow (\pi/4) \sec \theta^* - 2\ell^*$. However, because the lengths of these horizontal line segments remain bounded, we have enough information to argue that ϕ cannot degenerate to π . If this did happen, then $\text{Ext}_0(\Gamma_2) \rightarrow \infty$, but under these assumptions

we have $\text{Ext}_+(\Gamma_2) \rightarrow \delta < \infty$, as depicted in Figure 15. Specifically, we use the restricted subset $\Gamma'_2 \subset \Gamma_2$, consisting curves joining only the edges indicated. In either case, $\text{Ext}_+(\Gamma'_2) < \infty$, and so $\text{Ext}_+(\Gamma_2) \leq \text{Ext}_+(\Gamma'_2) < \infty$.

To show that ϕ cannot degenerate to 0, we first argue that $(\pi/4) \sec \theta - 2\ell$ cannot tend to 0. This is easily seen by appealing to the bilinear relation equations for $gdh \wedge dz$ and $(1/g)dh \wedge dz$ used in the proof of Lemma 2; assuming $(\ell, \theta, \alpha) \rightarrow (\ell^*, \theta^*, 0)$, $\phi \rightarrow 0$ and using equation (11), we find

$$\begin{aligned} -4\ell^* &= \frac{i\pi}{4 \sin \theta^* \cos \theta^*} \left(e^{i\theta^*} (a_1 - a_3) - e^{-i\theta^*} (a_2 - a_4) \right) \\ &= \frac{i\pi}{4 \sin \theta^* \cos \theta^*} \left((a_1 - a_3) \left(e^{i\theta^*} - e^{-i\theta^*} \right) \right) \\ &= \frac{i\pi}{\sin \theta^* \cos \theta^*} (a_1 - 1) (i \sin \theta^*) \\ \ell^* &= \frac{\pi}{4} \sec \theta^* (a_1 - 1). \end{aligned}$$

Here, as before, we made use of the relations $a_2 = e^{-2i\phi/a_1}$ and $a_3 = 1 + e^{i\phi} - a_1$. We conclude that the horizontal length vanishes if and only if $(a_1 - 1) = 1/2$ in the limit, which implies that $a_1 \rightarrow 3/2$. However, if we repeat this process with equation (12), we find

$$\ell^* = \frac{\pi}{4} \sec \theta^* (1 - a_1)$$

which implies that $a_1 \rightarrow 1/2$. Therefore, ϕ cannot tend to 0. By assumption, the parameter θ is likewise not degenerating. This leaves t to degenerate, which, as noted in Proposition 8, results in an unsolved period problem, yielding our desired contradiction. q.e.d.

We are now in a position to prove the following

Theorem 4. *Given any $\theta \in (0, \pi/2)$, there exists an immersed $S(1, 2\theta)$.*

Proof. From Lemma 2, we see that limiting flat structure triples of the form $(0, \alpha, \theta^*)$ are impossible. We have already remarked that if $\ell \rightarrow \infty$ then θ degenerates, without loss of generality, to 0. Moreover, Lemma 3 rules out the possibilities of $(\ell^*, 0, \theta^*)$ and $(\ell^*, \pi/2, \theta^*)$ as limit triples.

Because our original coordinates (ϕ, θ, t) must degenerate, our geometric coordinates must degenerate, too. Using these first three Lemmas and the fact that $\ell \rightarrow \infty \Rightarrow \theta \rightarrow 0$, though, we see that the only possible degenerations all include $\theta \rightarrow 0$. Hence, for every $\theta \in (0, \pi/4]$ we have an immersed $S(1, 2\theta)$. By Proposition 6, this set of allowable θ may be extended to $(0, \pi/2)$. q.e.d.

5.4. Step 2: Relating (ℓ, θ, α) and (ϕ, θ, t) . In this subsection we show that if ℓ degenerates to ∞ , then ϕ can not degenerate. This is the content of Lemma 4, and although it is similar in flavor to Lemma 1, the proof is more delicate. As a result, we are able to understand ℓ degenerating in terms of the quantity $|\operatorname{Im}(se^{i\phi})| \csc \theta \sec \theta$ degenerating to 0 or ∞ ; this is the content of Lemma 5.

Lemma 4. *If $\ell \rightarrow \infty$ then ϕ cannot degenerate.*

Proof. Without loss of generality, assume $\theta \rightarrow 0$. Because $(\pi/4) \sec \theta - 2\ell \cos \alpha > 0$, we have that $\alpha \rightarrow \pi/2$, and we also have the upper bound $2\ell \cos \alpha \leq \sec \theta \rightarrow 1$.

First we show that $\csc \theta / \ell \rightarrow \infty$. It is clear that $\operatorname{Ext}_-(\tilde{\Gamma}) \rightarrow 0$ as $(\ell, \theta, \alpha) \rightarrow (\infty, 0, \pi/2)$, where $\tilde{\Gamma}$ consists of curves enclosing the punctures a_1 and a_2 . This is easily verified by considering the subset $\tilde{\Gamma}' \subset \tilde{\Gamma}$ given by the depicted curves in Figure 16. The $(1/g)dh$ flat structure in Figure 16 has been rescaled by $1/\ell$, and the curves under consideration are only allowed to intersect the edges indicated.

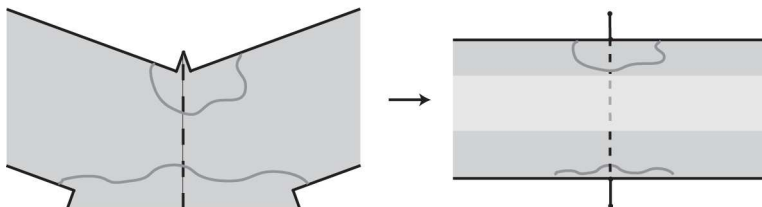


Figure 16. $\operatorname{Ext}_-(\tilde{\Gamma}') \rightarrow 0$

The length of the vertical line segment in Figure 16 is given by $2 \sin \alpha + (\pi/4) \csc \theta / \ell$, and so either tends to infinity or a positive value as $(\ell, \theta, \alpha) \rightarrow (\infty, 0, \pi/2)$. The length of the horizontal line segment is given by $2 \cos \alpha + (\pi/4) \sec \theta / \ell$ and hence tends to 0 under the assumed degeneration, as depicted in the diagrams.

As our parameters degenerate, the curves in $\tilde{\Gamma}'$ can be contained in arbitrarily small balls, implying that $\operatorname{Ext}_-(\tilde{\Gamma}') \rightarrow 0$. Of course, this implies that $\operatorname{Ext}_-(\tilde{\Gamma}) \rightarrow 0$.

However, if the ratio $\csc \theta / \ell$ does not tend to ∞ , then $\operatorname{Ext}_+(\Gamma)$ limits on a positive value. To see this, rescale the gdh flat structure by $1/\ell$, and note that $\tilde{\gamma} \in \tilde{\Gamma}$ must contain solid or dotted sub-arcs, like the ones depicted in Figure 17. Specifically, these sub-arcs pass through the darkly-shaded, polygonal region D .

D is a symmetric region, and as a set in \mathbb{E}^2 , one quarter of it is the polygonal region whose vertices coincide with the set of points

$$\left\{ \left(0, 2 \cos \alpha \right), \left(0, \frac{\pi \csc \theta}{4 \ell} \right), \left(\delta + 2 \sin \alpha, (\delta + 2 \sin \alpha) \tan \theta + \frac{\pi \csc \theta}{4 \ell} \right), \right. \\ \left. (2 \sin \alpha, 0), (2 \sin \alpha + \delta, 0) \right\}$$

where δ is an arbitrary, fixed positive number. Reflect this set across the real and imaginary axes and intersect the resulting polygonal domain with the *gdh* flat structure to obtain D , which is pictured in Figure 17 as a darkly shaded region.

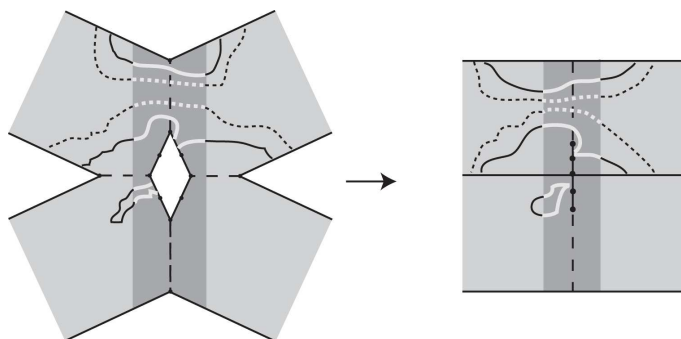


Figure 17. Dark region, D , carries the standard Euclidean metric

Equip these flat structures with the Euclidean metric on D ; that is, consider the metric ρ given by

$$\rho(z) = \begin{cases} 1 & \text{if } z \in D \\ 0 & \text{if } z \notin D \end{cases}$$

This choice of ρ provides us with a positive lower bound on the extremal length $\text{Ext}_+(\Gamma)$ (we have emphasized where our depicted curves intersect this region by highlighting sub-arcs with a lighter shade). This implies $\text{Ext}_+(\tilde{\Gamma}) > 0$.

Remark: The above picture assumes that the ratio $\csc \theta / \ell$ limits on a finite, positive value. If instead this limits to 0, then the Extremal Length $\text{Ext}_+(\tilde{\Gamma})$ tends to ∞ .

For the rest of the proof, we will assume $\csc \theta / \ell \rightarrow \infty$, which will be depicted in limiting, rescaled *gdh* structures via vertical line segments whose lengths increase without bound.

Again, we first argue that ϕ cannot degenerate to π . This follows because, again, $\text{Ext}_0(\Gamma_2) \rightarrow \infty$ under this degeneration, but $\text{Ext}_+(\Gamma_2) \rightarrow 0$

under the degeneration $(\ell, \theta, \alpha) \rightarrow (\infty, 0, \pi/2)$. This can be seen by using the set of curves Γ'_2 , used in the proof of Lemma 3, and rescaling the *gdh* flat structure by $1/\ell$.

We now show that ϕ cannot degenerate to 0. Consider the set $\hat{\Gamma}$, consisting of curves that enclose the points $1/2 + e^{i\phi}$, a_1 , a_2 , and $1 + e^{i\phi}/2$, but that do not intersect the line segment joining the origin to ω_3 . Such a curve is depicted in Figure 18.

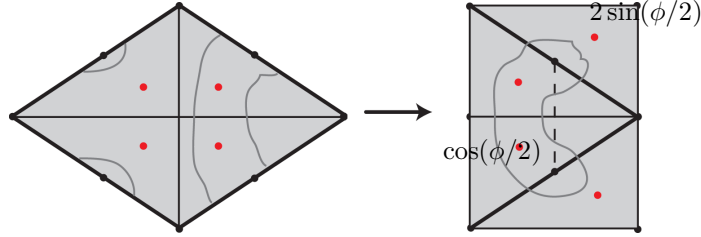


Figure 18. A curve in the set $\hat{\Gamma}$

After we rescale the torus by $\csc(\phi/2)$ and fix a neighborhood of the dotted line depicted in Figure 18, it is clear that the extremal length $\text{Ext}_0(\hat{\Gamma})$ increases without bound as $\phi \rightarrow 0$. This happens because the curves enclosing the half-period points are not allowed to intersect the bordering line segments of the identified rectangle in Figure 18 (on the right). As $\phi \rightarrow 0$ this rescaled rectangle becomes infinitely wide and, more to the point, every curve $\hat{\gamma} \in \hat{\Gamma}$ becomes “pinched,” which forces the extremal length to become infinite.

However, we can find a subset $\hat{\Gamma}' \subset \hat{\Gamma}$ that has $\text{Ext}_+(\hat{\Gamma}') \rightarrow 0$. Let $\hat{\Gamma}'$ denote the set of curves depicted in Figure 19. This figure shows the *gdh* flat structure (and its limit) rescaled by $1/\ell$. A curve $\hat{\gamma}' \in \hat{\Gamma}'$ is only allowed to cross the *gdh* geodesics joining 0 and ω_i ($i \in \{1, 2\}$) once, and it is also only allowed to cross the *gdh* geodesics joining ω_3 and the punctures once.

The limiting extremal length is zero since all limiting curves can be contained in arbitrarily small open balls. Hence, $\text{Ext}_+(\hat{\Gamma}) \leq \text{Ext}_+(\hat{\Gamma}') \rightarrow 0$, which contradicts the fact that $\text{Ext}_0(\hat{\Gamma}) \rightarrow \infty$. We are forced to conclude that ϕ cannot limit on 0, which completes the proof. q.e.d.

Lemma 5. *The following hold*

$$\ell \rightarrow 0 \iff \frac{|\text{Im}(se^{i\phi})|}{\sin \theta \cos \theta} \rightarrow 0$$

$$\ell \rightarrow \infty \iff \frac{|\text{Im}(se^{i\phi})|}{\sin \theta \cos \theta} \rightarrow \infty$$

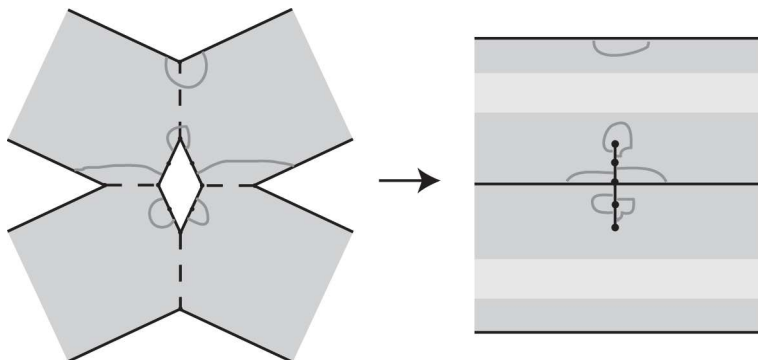


Figure 19. The set of curves $\hat{\Gamma}$

Proof. This follows simply by noting that

$$2\ell = \left| \int_0^1 gdh \right| = \frac{|\operatorname{Im}(se^{i\phi})|}{4 \sin \theta \cos \theta} \left(t \cdot \left| \int_0^1 \frac{\wp - e_3}{(\wp - s)(\wp - \bar{s}e^{-2i\phi})} dx \right| \right)$$

If $\ell \rightarrow 0$ or if $\ell \rightarrow \infty$, then ϕ cannot degenerate. After appealing to Proposition 8, we conclude that our original parameters (ϕ, θ, t) are limiting on $(\phi^*, 0, t^*)$. The fact that t and ϕ are not degenerating is enough to conclude that the parenthetical term in the above expression for ℓ remains bounded away from 0 and ∞ . Therefore, the only way for ℓ to vanish or blow up is if the coefficient $\operatorname{Im}(se^{i\phi}) \sec \theta \csc \theta$ does so. q.e.d.

5.5. Step 3: Producing the gdh Flat Structure for $\mathcal{H}(1)$. The main result in this section is that the parameter ℓ cannot degenerate. This is accomplished via Lemma 6, and it leaves only a handful of flat structures that, via more extremal length arguments, are easily dismissed as limits. The only “surviving” candidate coincides with the flat structure for $\mathcal{H}(1)$.

Lemma 6. *As $(\phi, \theta, t) \rightarrow (\phi^*, 0, t^*)$ the quantity $\operatorname{Im}(se^{i\phi}) \sec \theta \csc \theta$ cannot tend to 0. Moreover, ℓ cannot tend to ∞ .*

Proof. We begin with our equation that relates our parameters ϕ, θ, t and s :

$$\begin{aligned}
4e^{2i\theta} e^{i\phi} \frac{(s - e_1)(s - e_2)}{(s - e_3)} &= t^2 \\
e^{i\phi} \frac{(s - e_1)(s - e_2)(\bar{s} - \bar{e}_3)}{|s - e_3|^2} &= e^{-2i\theta} \frac{t^2}{4} \\
e^{-i\phi} (\bar{s} - \bar{e}_1)(\bar{s} - \bar{e}_2)(s - e_3) &= e^{2i\theta} \frac{t^2}{4} |s - e_3|^2 \\
e^{-i\phi} \bar{s} |s|^2 + \underline{e^{-i\phi} \bar{e}_3 |s|^2} + e^{i\phi} s |e_1|^2 - (e_3 \bar{s}) e^{-i\phi} s - |e_3|^2 e^{-i\phi} \bar{s} - \underline{e^{-i\phi} e_3 \bar{e}_1 e_2} \\
&= e^{2i\theta} \frac{t^2}{4} |s - e_3|^2
\end{aligned}$$

We now take an imaginary part of both sides, noting that the underlined terms are purely real. The imaginary part of the left hand side is therefore given by

$$\begin{aligned}
(13) \quad & \text{Im} (e^{-i\phi} \bar{s}) \cdot (|s|^2 - |e_3|^2) + \text{Im} (e^{i\phi} s) \cdot |e_1|^2 - \text{Im} (e^{-i\phi} s (e_3 \bar{s})) \\
&= \text{Im} (e^{-i\phi} \bar{s}) \cdot (|s|^2 - |e_3|^2) + \text{Im} (e^{i\phi} s) \cdot |e_1|^2 \\
(14) \quad & - \text{Im} (e^{-i\phi} \bar{s} (e_3 \bar{s}) + e^{-i\phi} \bar{s} (\bar{e}_3 s)) \\
(15) \quad &= \text{Im} (e^{i\phi} s) \cdot (|e_3|^2 - |s|^2 + |e_1|^2 - 2\text{Re}(e_3 \bar{s})) \\
(16) \quad &= \text{Im} (e^{i\phi} s) \cdot (-|s - e_3|^2 + 2|e_3|^2 + |e_1|^2) \\
(17) \quad &= \text{Im} (e^{i\phi} s) \cdot (|e_1 - e_3|^2 - |s - e_3|^2).
\end{aligned}$$

Because the expression $\text{Im} (e^{-i\phi} \bar{s} (\bar{e}_3 s)) = \text{Im} (e^{-i\phi} \bar{e}_3 |s|^2) = 0$, we are free to add it to equation (13) in order to obtain equation (14). Equation (17) is obtained from equation (16) by noting that

$$\begin{aligned}
|e_1 - e_3|^2 &= (e_1 - e_3) \overline{(e_1 - e_3)} = e^{2i\phi} (e_1 - e_3) (e_2 - e_3) \\
&= e^{2i\phi} (e_1 e_2 - e_3 (e_1 + e_2) + e_3^2) \\
&= e^{2i\phi} (e^{-2i\phi} |e_1|^2 - e_3 (-e_3) + e_3^2) = e^{2i\phi} (e^{-2i\phi} |e_1|^2 + 2e_3^2) \\
&= |e_1|^2 + 2|e_3|^2
\end{aligned}$$

Setting equation (17) equal to the imaginary part of $e^{2i\theta} \frac{t^2}{4} |s - e_3|^2$ gives

$$(18) \quad \text{Im} (e^{i\phi} s) \cdot (|e_1 - e_3|^2 - |s - e_3|^2) = 2 \sin \theta \cos \theta \cdot \frac{t^2}{4} |s - e_3|^2$$

$$(19) \quad \frac{\text{Im} (e^{i\phi} s)}{2 \sin \theta \cos \theta} \left(\frac{|e_1 - e_3|^2 - |s - e_3|^2}{|s - e_3|^2} \right) = \frac{t^2}{4}$$

$$(20) \quad \frac{4}{t^2} \frac{\text{Im} (e^{i\phi} s)}{2 \sin \theta \cos \theta} \left(\frac{|e_1 - e_3|^2}{|s - e_3|^2} - 1 \right) = 1.$$

Equation (20) implies that ℓ cannot tend to zero when $(\phi, \theta, t) \rightarrow (\phi^*, 0, t^*)$. For if $\ell \rightarrow 0$ then by Lemma 5 the quantity $\text{Im}(e^{i\phi_s}) \sec \theta \csc \theta \rightarrow 0$, too, violating (20).

Unfortunately, it is not easy to use the above expression to show that ℓ cannot tend to infinity. To demonstrate this, we use another extremal length argument. As we have already noted, if $\ell \rightarrow \infty$ then the torus parameter ϕ cannot degenerate; this was the content of Lemma 5, and as we recalled at the start of the proof for that Lemma, we know that $\alpha \rightarrow \pi/2$ and $\csc \theta/\ell \rightarrow \infty$ as $\ell \rightarrow \infty$.

The rest of the proof of Lemma 5 used the gdh flat structure to conclude that ϕ was not degenerating. Working with the $(1/g)dh$ flat structure, we show that, indeed, $\phi \rightarrow 0$, providing a desired contradiction.

Under the assumption that $(\ell, \theta, \alpha) \rightarrow (\infty, 0, \pi/2)$ and that $\csc \theta/\ell \rightarrow \infty$, we rescale the $(1/g)dh$ flat structure by ℓ and let the structure degenerate. We use a subset of $\Gamma'_2 \subset \Gamma_2$ of the homology class of the diagonal joining 1 and $e^{i\phi}$ on the underlying torus. The subset Γ'_2 consists of curves restricted to join the opposite sides of a rectangle of length A and height B where

$$A = 4 \cos \alpha + 2 \frac{\sec \theta}{\ell}, \quad B = 2 \sin \alpha$$

The set Γ'_2 is depicted in Figure 20, and its extremal length is given by

$$\text{Ext}_-(\Gamma'_2) = \frac{A}{B} = \frac{2 \cos \alpha + \frac{\sec \theta}{\ell}}{\sin \alpha} \rightarrow 0$$

which implies that $\text{Ext}_-(\Gamma_2) \rightarrow 0$.

We therefore have $\text{Ext}_-(\Gamma_2) \rightarrow 0 \Rightarrow \text{Ext}_0(\Gamma_2) \rightarrow 0 \Rightarrow \phi \rightarrow 0$, which is a contradiction. q.e.d.

Theorem 5. *As $\theta \rightarrow 0$ the surfaces $S(1, 2\theta) \rightarrow \mathcal{H}(1)$.*

Proof. We prove this by showing that the gdh flat structures for $S(1, 2\theta)$ converge to the gdh flat structure we claim represents $\mathcal{H}(1)$. The notion of convergence we are using is that of pointed, Gromov-Hausdorff (for more details, see [8]).

Previous lemmas demonstrate that ℓ cannot tend to 0 or ∞ . From Lemma 3 we know that α cannot degenerate in isolation. As a result, after assuming $\theta \rightarrow 0$, the only possible limits are $(\ell^*, 0, \alpha^*)$, $(\ell^*, 0, 0)$ and $(\ell^*, 0, \pi/2)$. If we can show that ϕ cannot degenerate, then the latter two cannot be possible. For even though $\theta \rightarrow 0$, the fact that $\ell \rightarrow \ell^* < \infty$ implies (by Lemma 5) that $\text{Im}(se^{i\phi})/\sin \theta$ remains bounded away from 0 and ∞ . As a result, the forms gdh and $(1/g)dh$ remain finite and well-defined, and under these conditions (as noted in Lemma 3), it is impossible for α to degenerate.

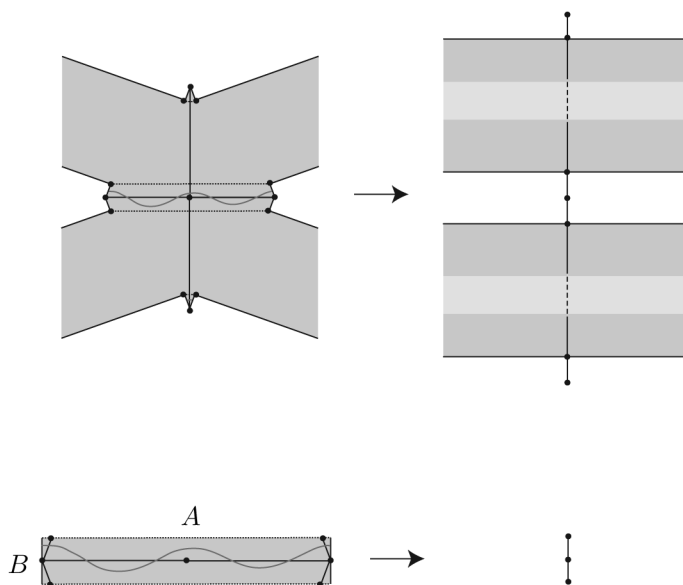


Figure 20. Γ'_2 on the $(1/g)dh$ flat structure

Consider $\text{Ext}_-(\Gamma_2)$ for the case $(\ell, \theta, \alpha) \rightarrow (\ell^*, 0, \pi/2)$, where, again, Γ_2 denotes the homology class of the diagonal joining 1 and $e^{i\phi}$ which, as we have already noted, develops to the horizontal line of symmetry for both flat structures. Using the $(1/g)dh$ flat structure, one finds that

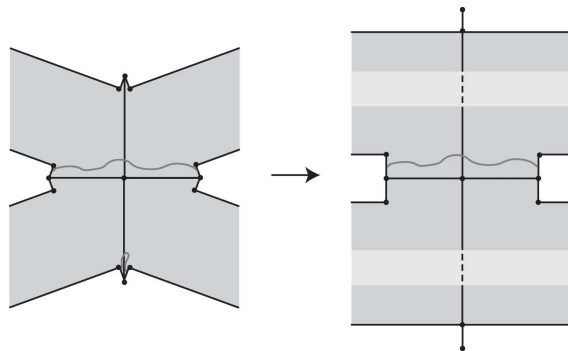


Figure 21. $\text{Ext}_-(\Gamma_2)$ remains positive and finite

this Extremal Length remains bounded away from 0 and ∞ , as depicted in Figure 21. Hence, ϕ cannot degenerate when $(\ell, \theta, \alpha) \rightarrow (\ell^*, 0, \pi/2)$.

Now suppose $(\ell, \theta, \alpha) \rightarrow (\ell^*, 0, 0)$. First we observe that $\text{Ext}_+(\Gamma_2) \rightarrow 0$. This is accomplished by using the subset $\Gamma'_2 \subset \Gamma_2$ depicted in Figure 22. Curves in this subset are symmetric, which is why we have

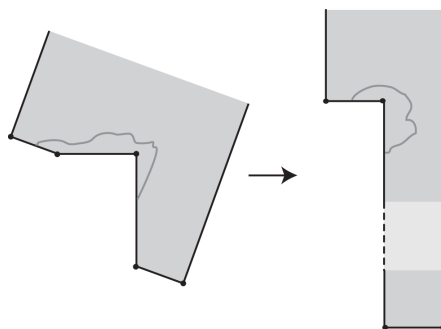


Figure 22. The set of curves $\Gamma'_2 \subset \Gamma_2$

depicted them on only one quarter of the structure. Moreover, on this quarter, these curves join the *gdh* geodesic joining 0 to ω_1 to the vertical line of symmetry, and they are not allowed to touch any other edge. We conclude that, if ϕ degenerates, then $\phi \rightarrow 0$. In this scenario, it is again true that $\text{Ext}_-(\tilde{\Gamma}) \rightarrow 0$, which implies that the punctures a_1 and a_2 are coming together, even after rescaling the torus by $\csc(\phi/2)$.

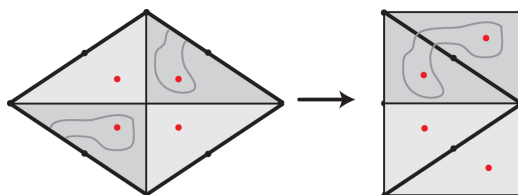


Figure 23. A curve in Γ^*

We now use the set Γ^* , given by curves enclosing a_1 and a_3 that enclose no other punctures or half-period points, and that are not allowed to cross any diagonal. Such a curve is depicted in Figure 23.

After rescaling the torus, we observe that $\text{Ext}_0(\Gamma^*) \rightarrow \infty$ either because the rescaled punctures tend infinitely far from each other, or because they limit on a diagonal; Figure 24 depicts how such a curve becomes “pinched.”

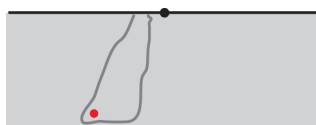


Figure 24. Piece of a curve $\gamma^* \in \Gamma^*$ getting pinched

However, $\text{Ext}_+(\Gamma^*)$ remains bounded away from infinity, since we may restrict to the subset of curves in the gdh flat structure depicted in Figure 25. Again, a curve in this subset is assumed to be symmetric and is only allowed to join the indicated edges (without intersecting any other edge).

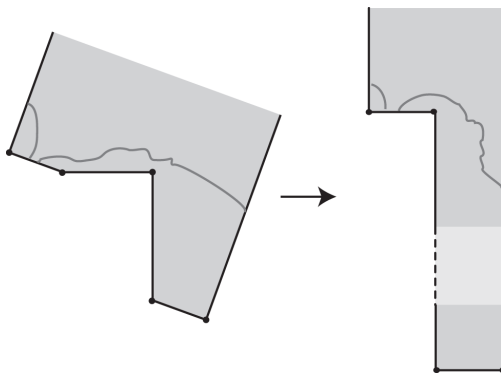


Figure 25. Subset of Γ^* with finite extremal length

Hence, ϕ cannot degenerate, which leaves the triple $(\ell^*, 0, \alpha^*)$ as a limit. This triple can correspond to two possible flat structures, though, depending on whether the quantity $\sec \theta - 2\ell \cos \alpha$ tends to 0 or something finite. If this quantity does vanish, it is easy to produce a contradiction. Specifically, $\text{Ext}_+(\Gamma_2) \rightarrow 0$ while $\text{Ext}_-(\Gamma_2) \rightarrow \delta > 0$. The former is made clear by restricting Γ_2 to the subset of curves depicted in Figure 26.

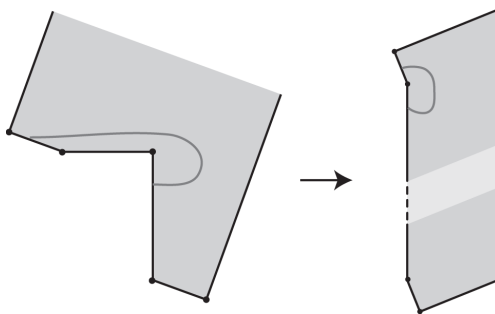


Figure 26. Subset of Γ_2

The latter is also clear via the following depiction of how $(1/g)dh$ degenerates. Every $\gamma \in \Gamma_2$ must join two ℓ -segments in the flat structure, as depicted below in Figure 27; the curves are only allowed to join the indicated edges without making contact with any other edges.

Also, these curves may wander more so than in the curve depicted in Figure 27.

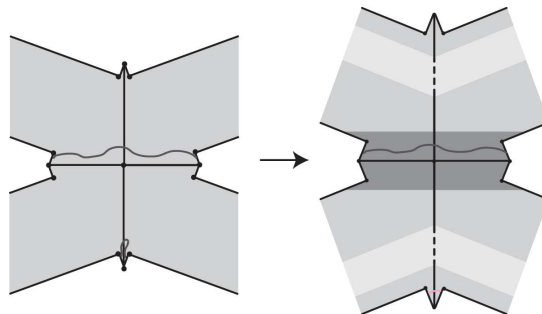


Figure 27. Darkly shaded region carries Euclidean metric

We equip the resulting structure with the Euclidean metric on the darkly shaded region, as was done in a previous example. More precisely, let D^* denote this symmetric, darkly shaded region; as a set in \mathbb{E}^2 , one quarter of D^* is the polygonal region whose vertices coincide with the set

$$\{(0, 0), (0, \delta + \ell \sin \alpha), (2\ell \cos \alpha \pi/4 \cdot \sec \theta, 0), (\ell \cos \alpha + \pi/4 \cdot \sec \theta, \ell \sin \alpha), (\delta + \ell \sin \alpha, \ell \cos \alpha + \pi/4 \cdot \sec \theta + \delta \tan \alpha)\}$$

where δ is an arbitrary but fixed positive constant.

D^* is obtained by reflecting this set across the real and imaginary axes and then intersecting with the $(1/g)dh$ flat structure. Using the Euclidean metric on D^* ,

$$\rho(z) = \begin{cases} 1 & \text{if } z \in D^* \\ 0 & \text{if } z \notin D^* \end{cases}$$

it is clear that every such γ has ρ -length bounded away from 0, and that the ρ -area of the structure remains finite. Hence, the extremal length remains bounded away from zero. We are forced to conclude that the gdh flat structure limits on $(\ell^*, 0, \alpha^*)$ with $1 - 2\ell^* \cos \alpha^* > 0$. We first cut and re-assemble the gdh flat structure as depicted in Figure 28.

We now let the structure degenerate, fixing the point in Figure 28 labeled p . What results is the gdh flat-structure for the genus one helicoid on its side, as depicted in Figure 29.

In order to finish the proof, we need to verify that this gdh flat structure implies that our limit surface $S(1, 0)$ has helicoidal ends. This certainly is believable, as the limiting flat structure is similar to the gdh flat structure for $\mathcal{H}(0)$.

As evidenced by this limiting flat structure, the form gdh did not degenerate, and so the same is true for the form $(1/g)dh$. As a consequence, the form $dh = (gdh \cdot (1/g)dh)^{1/2}$ did not degenerate, either.

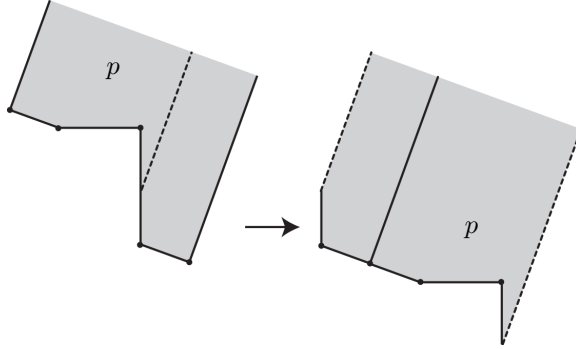


Figure 28. Reassembled gdh flat structure

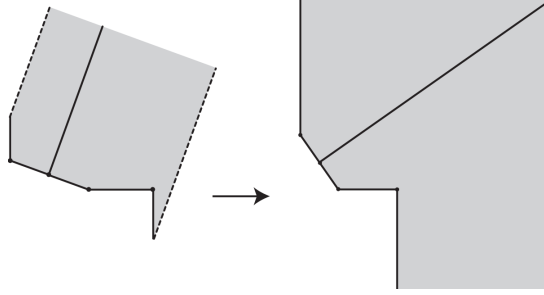


Figure 29. Limiting gdh flat structure

Because $dh(\phi, \theta, t)$ is given by

$$dh = \frac{\wp(a_1) - \wp(a_2)}{8 \sin \theta \cos \theta} \cdot \frac{d\wp}{(\wp - \wp(a_1))(\wp - \wp(a_2))},$$

as $\theta \rightarrow 0$ and $a_1 \rightarrow a_2$, the quotient $(\wp(a_1) - \wp(a_2))/(8 \sin \theta \cos \theta)$ necessarily tends to a finite value. This produces a well-defined, non-degenerate 1-form for the limiting height differential, which we notate as $dh_{\mathcal{H}}$:

$$dh_{\mathcal{H}(1)} = dh(\phi^*, 0, t^*) = k \cdot ie^{-i\phi} \cdot \frac{d\wp}{(\wp - \wp(a_1))^2}$$

where $k \in \mathbb{R}$. We similarly use the notation $g_{\mathcal{H}(1)}$ to denote the Gauss map for this limiting surface.

Consider the form $dz_1 = dz_1(\phi, \theta, t)$, which is given by

$$dz_1 = \frac{1}{2} \left(\frac{dh}{g} = gdh \right).$$

This form will play the role of the height differential for the upright, genus one helicoid when $\theta \rightarrow 0$. That is, dz_1 develops two simple poles

with purely imaginary residue at the punctures a_1 and a_3 at $\theta = 0$. The gauss map will take on the values $g_{\mathcal{H}(1)}(a_1) = 1$ and $g_{\mathcal{H}(1)}(a_3) = -1$ at the points a_1 and a_3 , points where $dh_{\mathcal{H}(1)}$ has double poles (and zero residue).

We need to establish two things: first, that the Gauss map is not branched over the values ± 1 and second, that dz_1 has purely imaginary residues at the punctures a_1, a_3 when $\theta = 0$. We accomplish both by computing the residues of dz_1 at the punctures a_1 and a_2 for each surface $S(1, 2\theta)$ and then taking a limit as $\theta \rightarrow 0$. If we let γ denote a loop enclosing both punctures a_1 and a_2 , then we find

$$R(\theta) = \int_{\gamma} dz_1 = \frac{i}{4} \sec \theta$$

$$\lim_{\theta \rightarrow 0} R(\theta) = \frac{i}{4}.$$

Similarly, near the puncture a_3 the form dz_1 has residue $-i/4$.

Because the surface we have produced should be the singly periodic genus one helicoid “on its side,” we use the adjusted Gauss map

$$G(z) = \frac{1 - g_{\mathcal{H}(1)}(z)}{1 + g_{\mathcal{H}(1)}(z)}$$

and focus attention on the data (G, dz_1) ; this data is used to produce an immersed surface in \mathbb{R} that, near the punctures a_i , is asymptotic to the upright (singly periodic) genus zero helicoid. The map is, as usual, given by

$$z \mapsto \operatorname{Re} \int^z \left(\frac{1}{2} \left(\frac{1}{G} - G \right) dz_1, \frac{i}{2} \left(\frac{1}{G} + G \right) dz_1, dz_1 \right) =: \operatorname{Re}(\phi_1, \phi_2, \phi_3)$$

To verify the asymptotics, we examine this data near the puncture a_1 (the puncture a_3 is handled via symmetry).

Near a_1 one can show that ϕ_i are given by

$$\begin{aligned} \phi_1(z) &= -kie^{-i\phi} \cdot \frac{h_{-2}}{z - a_1} + O(z - a_1) \\ &= -kie^{i\phi/2} |h_{-2}| \cdot \frac{1}{z - a_1} + O(z - a_1) \\ \phi_2(z) &= ke^{-i\phi} \cdot h_{-2} \frac{1}{z - a_1} + O(z - a_1) \\ &= ke^{i\phi/2} |h_{-2}| \cdot \frac{1}{z - a_1} + O(z - a_1) \\ \phi_3(z) &= \frac{1}{2} kie^{-i\phi} \cdot h_{-2} c_1 \log(z - a_1) + O(z - a_1) \\ &= \pm \frac{1}{2} k |h_{-2}| \cdot |c_1| \cdot i \log(z - a_1) + O(z - a_1) \end{aligned}$$

where for each expression we have chosen the constant of integration so that the holomorphic parts of each $\phi_i(z)$ vanish at $z = a_i$, and that $e^{-i\phi} \cdot h_{-2} \cdot c_1 \in \mathbb{R}$.

Shifting our coordinate z so that a_1 corresponds to the origin, we find

$$\begin{aligned}\phi_1 &\sim -\frac{kie^{i\phi/2}|h_{-2}|}{z} \\ \phi_2 &\sim \frac{ke^{i\phi/2}|h_{-2}|}{z} \\ \phi_3 &\sim \pm \frac{1}{2}k|h_{-2}| \cdot i|c_1| \log(z - a_1).\end{aligned}$$

Using polar coordinates for $z = re^{i\alpha}$, the triple $\text{Re}(\phi_1, \phi_2, \phi_3)$ is therefore asymptotic to

$$\text{Re}(\phi_1, \phi_2, \phi_3) \sim k|h_{-2}| \left(\frac{\sin(\phi/2 - \alpha)}{r}, \frac{\cos(\phi/2 - \alpha)}{r}, \mp |c_1| \alpha \right)$$

proving the existence of helicoidal ends.

Combined with [3], this is enough to establish our limit as the singly periodic, genus one helicoid. q.e.d.

5.6. Embeddedness. We are now in a position to prove the main theorem. All that is left to establish is that the surfaces $S(1, 2\theta)$ are embedded.

Proposition 9. *For every θ , the surface $S(1, 2\theta)$ is embedded.*

Proof. Let $T = \{\theta \in (0, \pi/4] : S(1, 2\theta) \text{ is embedded}\}$; we will now demonstrate that T is non-empty, open, and closed. Connectivity of the interval $(0, \pi/4]$ then implies that $T = (0, \pi/4]$.

Karcher [14] proved that $S(1, \pi/2)$ is embedded. Later, Weber-Wolf [27] proved that for any $g \geq 1$ the surfaces $S(g, \pi/2)$ are embedded. Hence, $\pi/4 \in T \Rightarrow T \neq \emptyset$.

We now show that T is open. Instead of working with the doubly periodic surfaces $S(1, 2\theta)$, we will work with a fundamental domain $\overline{S}(1, 2\theta) := S(1, 2\theta)/\Lambda$ where Λ is the 2-dimensional lattice generated by the two (period) vectors

$$\begin{aligned}\vec{v}_1 &= \frac{\pi}{2} (\sec \theta, -\csc \theta, 0) \\ \vec{v}_2 &= \frac{\pi}{2} (\sec \theta, \csc \theta, 0)\end{aligned}$$

Let \overline{T} denote the set of θ for which $\overline{S}(1, 2\theta)$ is embedded. Since $S(1, 2\theta)$ is embedded $\iff \overline{S}(1, 2\theta)$ is embedded, we have that $\overline{T} = T$, and so it suffices to show that \overline{T} is both open and closed.

Let $\theta_0 \in \overline{T}$. After translating and rotating the surface $\overline{S}(1, 2\theta_0)$, we can assume that a neighborhood of the puncture a_1 is asymptotic to

the vertical plane Π_1 defined below and, similarly, that a neighborhood of the puncture a_3 is asymptotic to the vertical plane Π_3 , obtained by shifting Π_1 a distance d along the x_1 -axis.

$$\Pi_1 = \{(x, x \cdot \tan \theta, z) : x, z \in \mathbb{R}\}$$

$$\Pi_3 = \{(x + d, x \cdot \tan \theta, z) : x, z \in \mathbb{R}\}$$

The quantity d is given by

$$d(\phi, \theta, t) = \left(\left(\int_{a_3}^{a_1} dx_1 \right)^2 + \left(\int_{a_3}^{a_1} dx_2 \right)^2 \right)^{1/2}$$

where, for instance, the path of integration can be taken as the union of the straight lines joining a_1 and a_3 to ω_3 , the center of the underlying torus.

Let $B(r)$ denote the ball of radius r

$$B(r) = \{(x, y, z) : x^2 + y^2 + z^2 \leq r^2\}$$

and let B_1 and B_2 denote its upper and lower hemispheres, respectively. Since d is continuous in (ϕ, θ, t) and, by assumption, $d(\phi_0, \theta_0, t_0) > 0$, this distance d remains positive for θ near θ_0 , so that $d \geq \eta > 0$ for some fixed constant η , for all θ near θ_0 . Hence, the corresponding surfaces $\overline{S}(1, 2\theta) \cap (\mathbb{R}^3 - B_1(r))$ are asymptotic to two vertical planes (Π_1 and Π_3) separated by a distance of at least $\eta > 0$. For large, fixed r and θ near θ_0 , $(\overline{S}(1, 2\theta) \cap (\mathbb{R}^3 - B_1(r)))$ consists of two components separated by a distance of $\delta > 0$, for some fixed δ . By symmetry, the same is true in the complement of the lower hemisphere $B_2(r)$.

Hence, the minimal surfaces $\overline{S}(1, 2\theta) \cap (\mathbb{R}^3 - B(r))$ remain embedded for θ near θ_0 . Because our curvature is uniformly bounded, continuity implies that the compact surfaces $\overline{S}(1, 2\theta) \cap B(r)$ remain embedded for θ near θ_0 , demonstrating that $\overline{T} = T$ is open.

A standard application of the maximum principle implies that T is closed. q.e.d.

Appendix A. Proof of Theorem 3

Using the notation

$$\hat{F}(\phi, \theta, t) = t^2 B(s(\phi, \theta, t)) + 4e^{2i\phi} C(s(\phi, \theta, t))$$

$$B(s) = \int_0^1 \frac{\wp - e_3}{(\wp - s)(\wp - \bar{s}e^{-2i\phi})} dz$$

$$C(s) = \int_0^1 \frac{\prod(\bar{\wp} - \bar{e}_i)}{(\bar{\wp} - \bar{s})(\bar{\wp} - se^{2i\phi})} d\bar{z}$$

$$\operatorname{Re}(\hat{F}) = R = t^2 \operatorname{Re} B + 4 \cos 2\phi (\operatorname{Re} C) - 4 \sin 2\phi (\operatorname{Im} C)$$

$$\begin{aligned}\operatorname{Im}(\hat{F}) &= I = t^2 \operatorname{Im}B + 4 \sin 2\phi (\operatorname{Re}C) + 4 \cos 2\phi (\operatorname{Im}C) \\ s(\phi, \theta, t) &= u(\phi, \theta, t) + iv(\phi, \theta, t)\end{aligned}$$

we derive explicit expressions that allow us to show $\det D\hat{F} \neq 0$ at p . First we differentiate R and I with respect to θ and t to obtain

$$\begin{aligned}\left. \frac{\partial R}{\partial t} \right|_p &= 2t (\operatorname{Re}B(s)) + t^2 \left(\frac{\partial \operatorname{Re}B}{\partial u} \frac{\partial u}{\partial t} + \frac{\partial \operatorname{Re}B}{\partial v} \frac{\partial v}{\partial t} \right) - 4 \left(\frac{\partial \operatorname{Re}C}{\partial u} \frac{\partial u}{\partial t} + \frac{\partial \operatorname{Re}C}{\partial v} \frac{\partial v}{\partial t} \right) \\ \left. \frac{\partial I}{\partial t} \right|_p &= 2t (\operatorname{Im}B(s)) + t^2 \left(\frac{\partial \operatorname{Im}B}{\partial u} \frac{\partial u}{\partial t} + \frac{\partial \operatorname{Im}B}{\partial v} \frac{\partial v}{\partial t} \right) - 4 \left(\frac{\partial \operatorname{Im}C}{\partial u} \frac{\partial u}{\partial t} + \frac{\partial \operatorname{Im}C}{\partial v} \frac{\partial v}{\partial t} \right) \\ \left. \frac{\partial R}{\partial \theta} \right|_p &= t^2 \left(\frac{\partial \operatorname{Re}B}{\partial u} \frac{\partial u}{\partial \theta} + \frac{\partial \operatorname{Re}B}{\partial v} \frac{\partial v}{\partial \theta} \right) - 4 \left(\frac{\partial \operatorname{Re}C}{\partial u} \frac{\partial u}{\partial \theta} + \frac{\partial \operatorname{Re}C}{\partial v} \frac{\partial v}{\partial \theta} \right) \\ \left. \frac{\partial I}{\partial \theta} \right|_p &= t^2 \left(\frac{\partial \operatorname{Im}B}{\partial u} \frac{\partial u}{\partial \theta} + \frac{\partial \operatorname{Im}B}{\partial v} \frac{\partial v}{\partial \theta} \right) - 4 \left(\frac{\partial \operatorname{Im}C}{\partial u} \frac{\partial u}{\partial \theta} + \frac{\partial \operatorname{Im}C}{\partial v} \frac{\partial v}{\partial \theta} \right).\end{aligned}$$

All of the expressions on the right side of the equal signs are evaluated at p . Note that many terms vanish because $\phi_0 = \pi/2$. Now let us collect expressions for the derivative of s with respect to t and θ . Using the equation relating ϕ, θ, t and s we find

$$4e^{2i\theta} e^{i\phi} \left(\frac{\partial s}{\partial t} (s - e_2) + (s - e_1) \frac{\partial s}{\partial t} \right) = 2t(s - e_3) + t^2 \frac{\partial s}{\partial t}$$

At the point $(\phi, \theta, s, t) = (\pi/2, \pi/4, t_0, s_0)$ this expression simplifies a great deal:

$$-\frac{\partial s}{\partial t} 8s_0 = 2t_0 s_0 + t_0^2 \frac{\partial s}{\partial t}$$

$$(21) \quad \frac{\partial s}{\partial t} = -\frac{2t_0 s_0}{t_0^2 + 8s_0} \in \mathbb{R}^-.$$

Similarly, we compute the partial with respect to θ and evaluate at $(\pi/2, \pi/4, t_0, s_0)$:

$$8ie^{2i\theta} e^{i\phi} (s - e_1)(s - e_2) + 4e^{2i\theta} e^{i\phi} \left(\frac{\partial s}{\partial \theta} (s - e_2) + \frac{\partial s}{\partial \theta} (s - e_1) \right) = t^2 \frac{\partial s}{\partial \theta}$$

$$8i(e_1^2 - s_0^2) - 8s_0 \frac{\partial s}{\partial \theta} = t_0^2 \frac{\partial s}{\partial \theta}$$

$$(22) \quad \frac{\partial s}{\partial \theta} = \frac{8i(e_1^2 - s_0^2)}{t_0^2 + 8s_0} \in i\mathbb{R}^+.$$

Because the partials s_t and s_θ are, respectively, purely real and imaginary, our expression for the partials of the real and imaginary parts of \hat{F} are nicely simplified. This follows from

$$(23) \quad \frac{\partial s}{\partial t} = \frac{\partial u}{\partial t}, \quad 0 = \frac{\partial v}{\partial t}$$

$$(24) \quad \frac{\partial s}{\partial \theta} = i \frac{\partial v}{\partial \theta}, \quad 0 = \frac{\partial u}{\partial \theta}.$$

Also, the partial I_t is simplified as, at this point, the imaginary parts of $B(s)$ and $C(s)$ are both zero. These observations yield the following equations

$$\begin{aligned} \frac{\partial R}{\partial t} \Big|_{\phi=\pi/2} &= 2t \operatorname{Re} B(s) + t^2 \frac{\partial \operatorname{Re} B}{\partial u} \frac{\partial u}{\partial t} - 4 \frac{\partial \operatorname{Re} C}{\partial u} \frac{\partial u}{\partial t} \\ \frac{\partial I}{\partial t} \Big|_{\phi=\pi/2} &= t^2 \frac{\partial \operatorname{Im} B}{\partial u} \frac{\partial u}{\partial t} - 4 \frac{\partial \operatorname{Im} C}{\partial u} \frac{\partial u}{\partial t} \\ \frac{\partial R}{\partial \theta} \Big|_{\phi=\pi/2} &= t^2 \frac{\partial \operatorname{Re} B}{\partial v} \frac{\partial v}{\partial \theta} - 4 \frac{\partial \operatorname{Re} C}{\partial v} \frac{\partial v}{\partial \theta} \\ \frac{\partial I}{\partial \theta} \Big|_{\phi=\pi/2} &= t^2 \frac{\partial \operatorname{Im} B}{\partial v} \frac{\partial v}{\partial \theta} - 4 \frac{\partial \operatorname{Im} C}{\partial v} \frac{\partial v}{\partial \theta}. \end{aligned}$$

We now differentiate B and C , each with respect to t and θ . To facilitate this process we first express the function $B(s)$ in terms of the real and imaginary parts of $s = u + iv$:

$$\begin{aligned} B(s) &= B(u, v) = \int_0^1 \frac{\wp - e_3}{(\wp - s)(\wp - \bar{s}e^{-2i\phi})} dx \\ &= \int_0^1 \frac{\wp - e_3}{\wp^2 - \wp(\bar{s}e^{-2i\phi} + s) + e^{-2i\phi}|s|^2} dx \\ &= \int_0^1 \frac{\wp - e_3}{\wp^2 - 2\wp e^{-i\phi}(u \cos \phi - v \sin \phi) + e^{-2i\phi}(u^2 + v^2)} dx \\ \frac{\partial B}{\partial u} &= - \int_0^1 \frac{(2ue^{-2i\phi} - 2\wp e^{-i\phi} \cos \phi)(\wp - e_3)}{(\wp^2 - 2\wp e^{-i\phi}(u \cos \phi - v \sin \phi) + e^{-2i\phi}(u^2 + v^2))^2} dx \\ \frac{\partial B}{\partial v} &= - \int_0^1 \frac{(2ve^{-2i\phi} + 2\wp e^{-i\phi} \sin \phi)(\wp - e_3)}{(\wp^2 - 2\wp e^{-i\phi}(u \cos \phi - v \sin \phi) + e^{-2i\phi}(u^2 + v^2))^2} dx. \end{aligned}$$

Evaluated at the point p —where, it bears reminding, the parameter $s_0 = u_0 + iv_0 = (u_0, v_0) = (u_0, 0)$ —these partials become

$$(25) \quad \left. \frac{\partial B}{\partial u} \right|_p = 2s_0 \int_0^1 \frac{\wp}{(\wp^2 - s_0^2)^2} dx \in \mathbb{R}^+$$

$$(26) \quad \left. \frac{\partial B}{\partial v} \right|_p = 2i \int_0^1 \frac{\wp^2}{(\wp^2 - s_0^2)^2} dx \in i\mathbb{R}^+$$

A similar series of computations is carried out for the function $C(s)$:

$$C(s) = C(u, v) = \int_0^1 \frac{(\prod \bar{\wp} - \bar{e}_i)}{(\bar{\wp}^2 - 2\bar{\wp}e^{i\phi}(u \cos \phi - v \sin \phi) + e^{2i\phi}(u^2 + v^2))} dx$$

$$\frac{\partial C}{\partial u} = - \int_0^1 \frac{(2ue^{2i\phi} - 2\bar{\wp}e^{i\phi} \cos \phi) (\prod \bar{\wp} - \bar{e}_i)}{(\bar{\wp}^2 - 2\bar{\wp}e^{i\phi}(u \cos \phi - v \sin \phi) + e^{2i\phi}(u^2 + v^2))^2} dx$$

$$\frac{\partial C}{\partial v} = - \int_0^1 \frac{(2ve^{2i\phi} + 2\bar{\wp}e^{i\phi} \sin \phi) (\prod \bar{\wp} - \bar{e}_i)}{(\bar{\wp}^2 - 2\bar{\wp}e^{i\phi}(u \cos \phi - v \sin \phi) + e^{2i\phi}(u^2 + v^2))^2} dx$$

Evaluating these expressions at p yields

$$(27) \quad \left. \frac{\partial C}{\partial u} \right|_p = 2s_0 \int_0^1 \frac{\wp^2 - e_1^2}{(\wp^2 - s_0^2)^2} dx \in \mathbb{R}^+$$

$$(28) \quad \left. \frac{\partial C}{\partial v} \right|_p = -2i \int_0^1 \wp \frac{\wp^2 - e_1^2}{(\wp^2 - s_0^2)^2} dx \in i\mathbb{R}^-.$$

With this information we can simplify the partials of R and I even further. Because taking real and imaginary parts commutes with partial differentiation (of real variables), we find that the imaginary parts of B_u and C_u along with the real parts of B_v and C_v are all zero. This leaves

$$\left. \frac{\partial R}{\partial t} \right|_p = 2t_0 B(s_0) + \frac{\partial u}{\partial t} \left(t_0^2 \frac{\partial B}{\partial u} - 4 \frac{\partial C}{\partial u} \right)$$

$$\left. \frac{\partial I}{\partial t} \right|_p = 0$$

$$\left. \frac{\partial R}{\partial \theta} \right|_p = 0$$

$$\left. \frac{\partial I}{\partial \theta} \right|_p = \frac{\partial v}{\partial \theta} \frac{1}{i} \left(t_0^2 \frac{\partial B}{\partial v} - 4 \frac{\partial C}{\partial v} \right)$$

The differential of our function \hat{F} at the point p therefore has determinant given by $R_t \cdot I_\theta$. Equations (22), (24), (26), and (28) imply that the above expression for $I_\theta(p) > 0$. We now focus our efforts on proving that $R_t(p) \neq 0$.

$$\begin{aligned} \frac{\partial R}{\partial t} \Big|_p &= 2t_0 B(s_0) + t_0^2 \frac{\partial u}{\partial t} \left(\frac{\partial B}{\partial u} - \frac{4}{t_0^2} \cdot \frac{\partial C}{\partial u} \right) \\ &= t_0 \left(2B(s_0) + t_0 \frac{\partial u}{\partial t} \left(\frac{\partial B}{\partial u} - \frac{4}{t_0^2} \cdot \frac{\partial C}{\partial u} \right) \right) \\ &= t_0 \left(B(s_0) - t_0 \cdot \frac{2t_0 s_0}{t_0^2 + 8s_0} \left(\frac{\partial B}{\partial u} - \frac{4}{t_0^2} \cdot \frac{\partial C}{\partial u} \right) \right) \end{aligned}$$

We now use the relations

$$\begin{aligned} t_0^2 &= \frac{4(e_1^2 - s_0^2)}{s_0} \\ t_0^2 + 8s_0 &= \frac{4(e_1^2 + s_0^2)}{s_0} \end{aligned}$$

to rewrite our expression for R_t . We have

$$\begin{aligned} \frac{\partial R}{\partial t} \Big|_p &= t_0 \left(2B(s_0) - 2s_0 \cdot \frac{e_1^2 - s_0^2}{e_1^2 + s_0^2} \left(\frac{\partial B}{\partial u} - \frac{4}{t_0^2} \cdot \frac{\partial C}{\partial u} \right) \right) \\ &= 2t_0 \left(B(s_0) - s_0 \cdot \frac{e_1^2 - s_0^2}{e_1^2 + s_0^2} \left(\frac{\partial B}{\partial u} - \frac{s_0}{e_1^2 - s_0^2} \cdot \frac{\partial C}{\partial u} \right) \right) \\ &= 2t_0 \left(B(s_0) - \left(s_0 \cdot \frac{e_1^2 - s_0^2}{e_1^2 + s_0^2} \cdot \frac{\partial B}{\partial u} - \frac{s_0^2}{e_1^2 + s_0^2} \cdot \frac{\partial C}{\partial u} \right) \right) \end{aligned}$$

The second term in the parentheses can be bounded above by $B(s_0)$. This follows directly from writing out this second term:

$$\begin{aligned} &s_0 \cdot \frac{e_1^2 - s_0^2}{e_1^2 + s_0^2} \cdot \frac{\partial B}{\partial u} - \frac{s_0^2}{e_1^2 + s_0^2} \cdot \frac{\partial C}{\partial u} \\ &= 2s_0^2 \cdot \frac{e_1^2 - s_0^2}{e_1^2 + s_0^2} \int_0^1 \frac{\wp}{(\wp^2 - s_0^2)^2} dx + \frac{2s_0^3}{e_1^2 + s_0^2} \int_0^1 \frac{e_1^2 - \wp^2}{(\wp^2 - s_0^2)^2} dx \\ &= \frac{2s_0^2}{e_1^2 + s_0^2} \left((e_1^2 - s_0^2) \int_0^1 \frac{\wp}{(\wp^2 - s_0^2)^2} dx + s_0 \int_0^1 \frac{e_1^2 - \wp^2}{(\wp^2 - s_0^2)^2} dx \right) \\ &= \frac{2s_0^2}{e_1^2 + s_0^2} \left(\int_0^1 \frac{e_1^2 \wp - s_0^2 \wp + s_0 e_1^2 - s_0 \wp^2}{(\wp^2 - s_0^2)^2} dx \right) \end{aligned}$$

The numerator in the final term is easy to bound. Recall that $0 < s_0 < e_1 < \wp$ along the path of integration. We therefore bound

$$s_0 e_1^2 - s_0 \wp^2 < s_0 e_1^2 - s_0 e_1^2 = 0$$

so that the numerator is bounded by $e_1^2\wp - s_0^2\wp = (e_1^2 - s_0^2)\wp$. In addition, we have

$$\frac{1}{\wp^2 - s_0^2} < \frac{1}{e_1^2 - s_0^2}$$

from which we conclude that the above expression is bounded above by

$$\frac{2s_0^2}{e_1^2 + s_0^2} \int_0^1 \frac{\wp(e_1^2 - s_0^2)}{(\wp^2 - s_0^2)(e_1^2 - s_0^2)} dx = \frac{2s_0^2}{e_1^2 + s_0^2} \int_0^1 \frac{\wp}{\wp^2 - s_0^2} dx$$

Finally, the coefficient in front of the integral is easily bounded by 1 since

$$e_1^2 + s_0^2 > s_0^2 + s_0^2 = 2s_0^2.$$

All together, this implies

$$\left(s_0 \cdot \frac{e_1^2 - s_0^2}{e_1^2 + s_0^2} \cdot \frac{\partial B}{\partial u} - \frac{s_0^2}{e_1^2 + s_0^2} \cdot \frac{\partial C}{\partial u} \right) < \int_0^1 \frac{\wp}{\wp^2 - s_0^2} dx = B(s_0).$$

This shows that $R_t(p) > 0$. Combined with the fact that $I_\theta(p) > 0$ we find that $\det D\hat{F}_{(\theta,t)}(p) > 0$, as claimed. q.e.d.

Appendix B. Proof of Proposition 7

Proposition 7 The function $s(\phi, \theta, t)$ is analytic in \mathcal{P} .

Proof. From the equation relating s to the variables ϕ, θ , and t we have that $s(\phi, \theta, t)$ is given by

$$\frac{-(4e^{2i\theta} e^{i\phi} e_3 - t^2) \pm \sqrt{(4e^{2i\theta} e^{i\phi} e_3 - t^2)^2 - 16e^{2i\theta} e^{i\phi} (4e^{2i\theta} e^{i\phi} e_1 e_2 + t^2 e_3)}}{8e^{2i\theta} e^{i\phi}}$$

This will depend analytically on θ, ϕ , and t provided the discriminant does not vanish. Observe that on the square torus, this expression becomes

$$\frac{1}{8} \left(\sqrt{t_0^4 + 64e_1^2} - t_0^2 \right)$$

For an arbitrary choice of $(\phi, \theta, t) \in \mathcal{P}$, the discriminant vanishes if and only if

$$\begin{aligned} t^4 - 24e^{2i\theta} e^{i\phi} e_3 t^2 + 16e^{4i\theta} e^{2i\phi} (e_3^2 - e_1 e_2) &= 0 \\ t^4 - 48e^{2i\theta} \operatorname{Re} \left(e^{i\phi} e_1 \right) t^2 + 16e^{4i\theta} e^{2i\phi} (e_1^2 + e_1 e_2 + e_2^2) &= 0 \\ t^4 - 48e^{2i\theta} \operatorname{Re} \left(e^{i\phi} e_1 \right) t^2 + 16e^{4i\theta} \left(2\operatorname{Re} \left(e^{2i\phi} e_1^2 \right) + |e_1|^2 \right) &= 0 \end{aligned}$$

From this we can solve for t^2 , which will be given by

$$\frac{48e^{2i\theta}\operatorname{Re}(e^{i\phi}e_1) \pm \sqrt{48^2e^{4i\theta}\operatorname{Re}(e^{i\phi}e_1)^2 - 64e^{4i\theta}(2\operatorname{Re}(e^{2i\phi}e_1^2) + |e_1|^2)}}{2}$$

$$= \frac{e^{2i\theta}}{2} \left(\operatorname{Re}(e^{i\phi}e_1) \pm \sqrt{48^2\operatorname{Re}(e^{i\phi}e_1)^2 - 64(2\operatorname{Re}(e^{2i\phi}e_1^2) + |e_1|^2)} \right)$$

We now analyze the expression in the radical above. The first term is clearly positive, and we next argue that the second term is positive as well. First, when $\phi = \pi/2$ the second term is $64(-e_1^2) < 0$. If this term ever vanishes for some value of ϕ we would have

$$2\operatorname{Re}\left((e^{i\phi}e_1)^2\right) = -|e_1|^2 = -|e^{i\phi}e_1|^2$$

$$2(u^2 - v^2) = -u^2 - v^2$$

$$3u^2 = 0$$

where we have notated $e^{i\phi}e_1 = u + iv$. In particular, this term vanishes if and only if $e^{i\phi}e_1$ is purely imaginary. However, this would imply

$$e_1 = \rho ie^{-i\phi} \Rightarrow e_2 = e^{-2i\phi}\overline{e_1} = -e_1$$

$$\Rightarrow 0 = e_1 + e_2 = -e_3 \Rightarrow \phi = \pi/2$$

which is a contradiction. Therefore, this term never changes sign, no matter the value of ϕ . As a consequence, the expression in the radical is a non-negative real number, and so we have that $t^2 = e^{2i\theta}K$ for some $K \in \mathbb{R}$. This is only possible if $\theta = 0, \theta = \pi/2$, or K and hence $t^2 = 0$. Of course, this only happens on the boundary of \mathcal{P} , not in the interior, which finishes the proof. q.e.d.

References

- [1] L. Ahlfors. *Lectures on Quasiconformal Mappings*, Van Nostrand, New York, 1966, MR 2241787, Zbl 1103.30001.
- [2] L. Ahlfors, *Conformal invariants: topics in geometric function theory*, McGraw-Hill Book Co., New York, 1973, MR 0357743.
- [3] A. Alarcón, L. Ferrer & F. Martin, *A uniqueness theorem for the singly periodic genus-one helicoid*, Trans. AMS **359** (6), 285–301, 2007, MR 2286058, Zbl 1121.53004.
- [4] F. Baginski & V. Ramos-Batista, Solving period problems for minimal surfaces with the support function, preprint.
- [5] P. Byrd & M. Friedman, *Handbook of Elliptic Integrals for Engineers and Physicists*, Springer-Verlag, Berlin-Göttingen-Heidelberg, 1954, MR 0595077, Zbl 0055.11905.
- [6] K. Chandrasekharan, *Elliptic Functions*, Springer-Verlag, New York, 1985, MR 0808396.

- [7] U. Dierkes, S. Hildebrandt, A. Küster & O. Wohlrab, *Minimal Surfaces I*, Grundlehren der mathematischen Wissenschaften 296, Springer-Verlag, 1992, MR 1215267.
- [8] M. Gromov, *Metric Structures for Riemannian and non-Riemannian Spaces*, Birkhäuser, Boston, MA, 1999, MR 2307192, Zbl 1113.53001.
- [9] R. Hardt, *Sullivan's local euler characteristic theorem*, Manuscripta Math. **12**, 87–92, 1974, MR 0338431, Zbl 0281.32005.
- [10] L. Hauswirth & M. Traizet, *The space of embedded doubly periodic minimal surfaces*, Indiana University Mathematics Journal **51**(5), 1041–1080, 2002.
- [11] D. Hoffman, H. Karcher & F. Wei, *Adding handles to the helicoid*, Bulletin of the AMS, New Series **29**(1), 77–84, 1993, MR 1193537, Zbl 0787.53003.
- [12] D. Hoffman, H. Karcher & F. Wei, *The genus one helicoid and the minimal surfaces that led to its discovery*, in *Global Analysis and Modern Mathematics*, Publish or Perish Press, 1993, K. Uhlenbeck, ed., 119–170.
- [13] W.H. Meeks III & J. Pérez, *The classical theory of minimal surfaces*, preprint.
- [14] H. Karcher, *Embedded minimal surfaces derived from Scherk's examples*, Manuscripta Math. **62**, 83–114, 1988, MR 0958255.
- [15] W.H. Meeks III & H. Rosenberg, *The geometry of periodic minimal surfaces*, Comment. Math. Helvetici **68**, 538–578, 1993, MR 1241472, Zbl 0807.53049.
- [16] W.H. Meeks III & M. Wolf, *Minimal surfaces with the area growth of two planes: the case of infinite symmetry*, J. Amer. Math. Soc. **20**(2), 441–465, 2007, MR 2276776, Zbl 1115.53008.
- [17] S. Montiel & A. Ros, *Schrödinger operators associated to a holomorphic map*, in *Proceedings Conference on Global Differential Geometry and Global Analysis*, volume 1841, pp. 147–174, Berlin, 1991, Lecture Notes in Mathematics, MR 1178529, Zbl 0744.58007.
- [18] S. Nag, *The Complex Analytic theory of Teichmüller Space*, Wiley, New York, 1988, MR 0927291.
- [19] R. Osserman, *A Survey of Minimal Surfaces*, Dover Publications, New York, 2nd edition, 1986, MR 0852409, Zbl 0209.52901.
- [20] H. Rosenberg & E. Toubiana, *Complete minimal surfaces and minimal horizons*, Journal of Differential Geometry **28**, 115–132, 1988, MR 0950557, Zbl 0657.53004.
- [21] H. F. Scherk, *Bemerkungen über die kleinste Fläche Innerhalb gegebener Grenzen*, J. R. Angew. Math. **13**, 185–208, 1835.
- [22] M. Troyanov, *Les surfaces euclidienne à singularités coniques*, L'Enseignement Mathématique **32**, 79–94, 1986, MR 0850552.
- [23] M. Weber, *The genus one helicoid is embedded*, Habilitationsschrift Bonn, 2000.
- [24] M. Weber, *Classical Minimal Surfaces in Euclidean Space by Examples: Geometric and Computational Aspects of the Weierstrass Representation*, volume 2 of *Clay Mathematics Proceedings*, pp. 19–62, American Mathematical Society, Providence, RI, 2001, MR 2167255, Zbl 1100.53015.
- [25] M. Weber, D. Hoffman & M. Wolf, *An embedded genus one helicoid*, Annals of Math. **169**, 347–448, 2009, MR 2480608, Zbl pre05578747.
- [26] M. Weber & M. Wolf, *Handle Addition for Doubly-Periodic Scherk Surfaces*, Journal of Differential Geometry, to appear.

- [27] M. Weber & M. Wolf, *Teichmüller theory and handle addition for minimal surfaces*, *Annals of Math.* **156**, 713–795, 1998, MR 1954234, Zbl 1028.53009.

MATHEMATICS AND COMPUTER SCIENCE DEPARTMENT
ST. MARY'S COLLEGE OF MARYLAND
18952 E. FISHER ROAD
ST. MARY'S CITY, MD, 20686-3001
E-mail address: cjdouglas@smcm.edu